

Phosphorus removal using an algae bacterial consortium in photo sequencing batch reactor(PSBR)

by

Joseph Mathew

A thesis submitted in partial fulfillment of the requirements for the Degree of Master of Engineering in Urban Water Engineering and Management at the Asian Institute of Technology and the degree of Master of Science at the UNESCO-IHE

Examination Committee: Dr. Thammarat Koottatep (Chairperson)
Dr. Peter Van Der Steen (Co-chair)
Prof. Ajit Annachhatre
Dr. Sangam Sherstha

Nationality: INDIAN

Previous Degree: Bachelor of Technology in Civil Engineering
National Institute of Technology,
Raipur, India

Scholarship Donor: Gates Foundation / UNESCO-IHE

Asian Institute of Technology
School of Environment Resource and Development
Thailand
May 2017

TABLE OF CONTENTS

CHAPTER	TITLE	PAGE
	Title Page	i
ABTRACT	iv	
LIST OF FIGURES		v
LIST OF TABLES		vi
List of Abbrviations		vii
1.	INTRODUCTION	8
	1.1. Background	8
	1.2. Statement of the problem	11
	1.3. Objectives	11
	1.3.1. Overall Objective	11
	1.3.2. Specific Objectives	11
	1.4. Scope	12
	1.5. Limitations	12
	1.6. Assumptions	12
2.	LITERATURE REVIEW	13
	2.1. Algal-Bacterial symbiotic photo bioreactor	13
	2.1.1. Algal communities	14
	2.1.2. Bacterial Communities	14
	2.2. Carbonate Alkalinity	15
	2.2.1. Alkalinity	17
	2.3. Calcium phosphate precipitation	19
	2.3.1. Effect of Carbonate in calcium phosphate precipitation	22
	2.4. Phosphorus uptake by algae	24
	2.5. Enhanced Biological Phosphorus Removal	26
	2.6. Biological nitrogen removal	27
	2.7. Artificial illumination	28
3.	METHODOLOGY	30
	3.1. Conceptual Framework	30
	3.2. Preparation of experiment	30
	3.2.1. Synthetic wastewater	30
	3.3. Microalgae cultivation	32
	3.4. Light Source	33
	3.5. Lab Scale Photo Sequencing Batch Reactor (PSBR)	33
	3.6. Sampling	38

3.7.	Modelling Chemical Speciation	39
3.8.	Calculations	40
3.8.1.	Alkalinity Mass Balance	40
3.8.2.	Ammonia Mass Balance	41
3.8.3.	Minimum Sludge Retention Time	42
4.	Result and Discussion	43
4.1.	Reactor 1 and 2: Biomass growth and environmental conditions	43
4.2.	Alkalinity Consumption rate	45
4.3.	Ammonium removal rate in PSBR	52
4.4.	Effect of solution condition on precipitation of calcium phosphate	56
4.5.	Phosphorus removal	63
4.6.	Discussion	67
5.	Conclusions and Recommendations	69
5.1.	Conclusions	69
5.2.	Recommendations	70
6.	REFERENCES	71
7.	APPENDIX 1	75

ABSTRACT

In the cycle of matter, the phosphorus has a slow cycle thus for the development of agriculture and industrial sector it's been mined from the phosphate rock reserves. An urgent need has arisen to close the phosphorus cycle by recovering and recycling it from the municipal wastewater which otherwise pollute the waterbodies. When the municipal wastewater is treated with an anaerobic digester there is a high concentration of inorganics such as bicarbonates, ammonia and phosphate observed.

The research study aims to recover/recycle phosphorus in the mixed liquor of PSBR via precipitation in form of calcium phosphate. The effluent coming from the anaerobic digester is treated using Photo sequencing Batch Reactor (PSBR). In situ photo oxygenation by algae in PSBR helps bacteria to remove COD and ammonia under controlled conditions.

To achieve calcium phosphate precipitation, high pH is required which may affect the nitrifying biomass in PSBR. The effect of pH increase in nitrifying biomass was studied by setting up two reactor wherein reactor 1 was kept at uncontrolled pH in the latter part of react stage and reactor 2 was kept at controlled pH throughout the study period. Two PSBRs were setup with inoculum of algae obtained from AIT pond and sludge inoculum obtained from sludge of AIT sewage treatment plant. Synthetic wastewater was used as influent for both the reactor having characteristic similar to effluent from anaerobic digester.

Ammonium removal rate of 2.53 ± 0.93 mg N-NH₃/L/hr in Reactor 1 and 2.25 ± 0.28 mg N-NH₃/L/hr in Reactor 2 was observed. The pH controller was switched off in Reactor 1 during Phase 2 and allowing photosynthesis of algae to biologically increase pH when alkalinity was low in the latter part of the react stage. A pH of 8.5 and 9 were achieved at the end of react stage by varying the light intensity of led light. Calcium chloride was dosed to the reactor and allowed to settle for 30 mins. Phosphorus removal efficiency of $74.31\% \pm 19\%$ at pH 9 and $25.64\% \pm 7\%$ at pH 8 was observed. Thus biologically and chemically induced phosphorus removal/recovery was achieved in the reactor without affecting the nitrification process.

LIST OF FIGURES

FIGURE	TITLE	PAGE
Figure 1	Countries with phosphorus reserves and countries that are importers of phosphate rocks(De Ridder, Jong, Polchar, & Lingemann, 2012)	8
Figure 2	Phosphorus Cycle(UNEP Year Book 2011)	9
Figure 3	Buffer index as a function of pH for a solution of the carbonate system(Conc:10 mmol/l) in water	16
Figure 4	Schematic of phosphorus recovery and removal from liquid scheme	24
Figure 5	A schematic representation of different P pools and fluxes inside and outside of an algae cell(Solovchenko, et.al , 2016).....	25
Figure 6	A schematic representation of phosphorus accumulating organism	26
Figure 7	Spectrum absorption efficiency of Chlorophyll a and b(Raven et al. 1976).....	28
Figure 8	Algae culture using LED lights.....	32
Figure 9	PSBRs illuminated using red led light during react stage.....	33
Figure 10	PSBRs Setup during the study period	34
Figure 11	Phase 2b: Operation Cycle of Reactor 1	36
Figure 12	Phase 2b: Operation Cycle of Reactor 2	37
Figure 13	Algae Bacteria-Initial Composition	43
Figure 14	Algae bacteria flocs formation during the study Phase 1[30],Phase 2.....	44
Figure 15	Suspended solids in Reactor 1 during Phase 1(30days), Phase 2a(6 days) and Phase 2b(10 Days)	44
Figure 16	Suspended solids in Reactor 2 during Phase 1(16days), Phase 2a(6 days) and Phase 2b(10 Days)	45
Figure 17	Measured Alkalinity in Reactor 1 during the study period	48
Figure 18	Measured Alkalinity in Reactor 2 during the study period	49
Figure 19	Alkalinity consumption in Reactor 1 during the study period	50
Figure 20	Alkalinity consumption in Reactor 2 during the study period	51
Figure 21	Ammonium Removal rate in Reactor 1 during the study period	53
Figure 22	Ammonium removal rate in Reactor 2 during the study period.....	54
Figure 23	Typical pH decrease graph observed due to nitrification.....	55
Figure 24	Nitrite Conc. in PSBRs during Phase 2b.....	56
Figure 25	Typical Temperature profile during the study period	57
Figure 26	Phosphorus Concentration in PSBR during Phase 2a	63
Figure 27	Typical pH increase achieved in Reactor 1 during Phase2b	64
Figure 28	Phosphorus Conc. at different React Period in Reactor 1 during Phase 2b	65
Figure 29	Phosphorus Conc. at different React Period in Reactor 2 during Phase 2b	65

LIST OF TABLES

TABLE	TITLE	PAGE
Table 1	Calcium phosphate phases.....	19
Table 2	Overview of various light sources (Blanken.W et.al ,2013)	28
Table 3	Synthetic wastewater used as influent for PSBRs during Phase 1 and 2	31
Table 4	Ogawa Trace element solution	32
Table 5	Detail of operational cycle in PSBRs	35
Table 6	Sampling Schedule during different phases	38
Table 7	Analytical Methods	38
Table 8	Composition of Algae Bacteria	43
Table 9	Alkalinity consumption rate (mgCaCO ₃ /L/hr) in PSBR	46
Table 10	Ammonium Removal rate in PSBRs.....	52
Table 11	Solid species: Specified log activity and Enthalpy.....	56
Table 12	Phase 2a: Stoichiometric matrix components and species at 0hr React Time	58
Table 13	Phase 2a: Stoichiometric matrix components and species at 11hr React Time ...	58
Table 14	Phase 2b: Stoichiometric matrix components and species at 0hr React Time	59
Table 15	Phase 2b: Stoichiometric matrix components and species at 11hr React Time ...	59
Table 16	Saturation Index and Mineral Components of PSBR in Phase2a at React Time 0 hr	60
Table 17	Saturation Index and Mineral Components of PSBR in Phase2a at React Time 11 hr.....	60
Table 18	Distribution of Components between dissolved and precipitated phases of PSBR in Phase2 at React Time 0	60
Table 19	Distribution of Components between dissolved and precipitated phases of PSBR in Phase2 at React Time 11	61
Table 20	Saturation Index and Mineral Components of PSBR in Phase2b at React Time 0 hr	62
Table 21	Saturation Index and Mineral Components of PSBR in Phase2b at React Time 11 hr.....	62
Table 22	Distribution of Components between dissolved and precipitated phases of PSBR in Phase2b at React Time 0	62
Table 23	Distribution of Components between dissolved and precipitated phases of PSBR in Phase2b at React Time 11	63
Table 24	Phosphorus removal efficiency observed in Reactor 1 during Phase 2b.....	66
Table 25	Phosphorus Removal Efficiency achieved in Reactor 2 during Phase 2b.....	66
Table 26	Phosphorus Removal Efficiency in PSBR with different pH achieved at the end of React Period during Phase 2b.....	67

List of Abbreviations

ACP	Amorphous calcium phosphate
AIT	Asian Institute of Technology
BNR	Biological Nitrogen Removal
COD	Chemical Oxygen Demand
DCPA	Monetite
DCPD	Brushite
DO	Dissolved Oxygen
EBPR	Enhanced Biological Phosphorus Removal
HAP	Hydroxyapatite
HRAP	High Rate Algae Pond
HRT	Hydraulic Retention Time
IP	Ionic activity Product
ISS	Inorganic Suspended Solids
LED	Light Emitting Diode
MAP	Magnesium Ammonium Phosphate
NH ₄ -N	Ammonia Nitrogen
NO ₃ -N	Nitrate Nitrogen
OCP	Octa calcium phosphate
PBR	Photo Bio Reactor
PSBR	Photo sequencing Batch Reactor
SI	Saturation Index
SRT	Sludge Retention Time
STP	Sewage Treatment Plant
TCP	Tri calcium phosphate
TSS	Total Suspended Solids
UNEP	United Nation Environment Programme
VSS	Volatile Suspended Solids
WW	Wastewater

CHAPTER

1. INTRODUCTION

1.1. Background

Phosphorus is an important element in the development of agriculture and industrial sectors. Unlike other elements in the matter cycle, phosphorus has a very slow cycle because it cannot attain gaseous state. Normally phosphorus is found as phosphate salts in rock formation and ocean sediment. The phosphate rock reserves are limited to very few countries. Most of the mined phosphate is used as fertilizer. The phosphates are exported to highly populated and agrarian economy as shown in Figure 1. There is a need to recover the phosphate and hence close the loop to be sustainable. However its release to surface water in agricultural runoff, domestic and industrial wastewater has led to high concentration in receiving water promoting eutrophication and subsequent ecological deterioration. Phosphorus must therefore be removed also from domestic and industrial effluents before dispersion and dilution to the environment which has made phosphorus removal and recovery, one of the focus areas in the field of wastewater treatment.

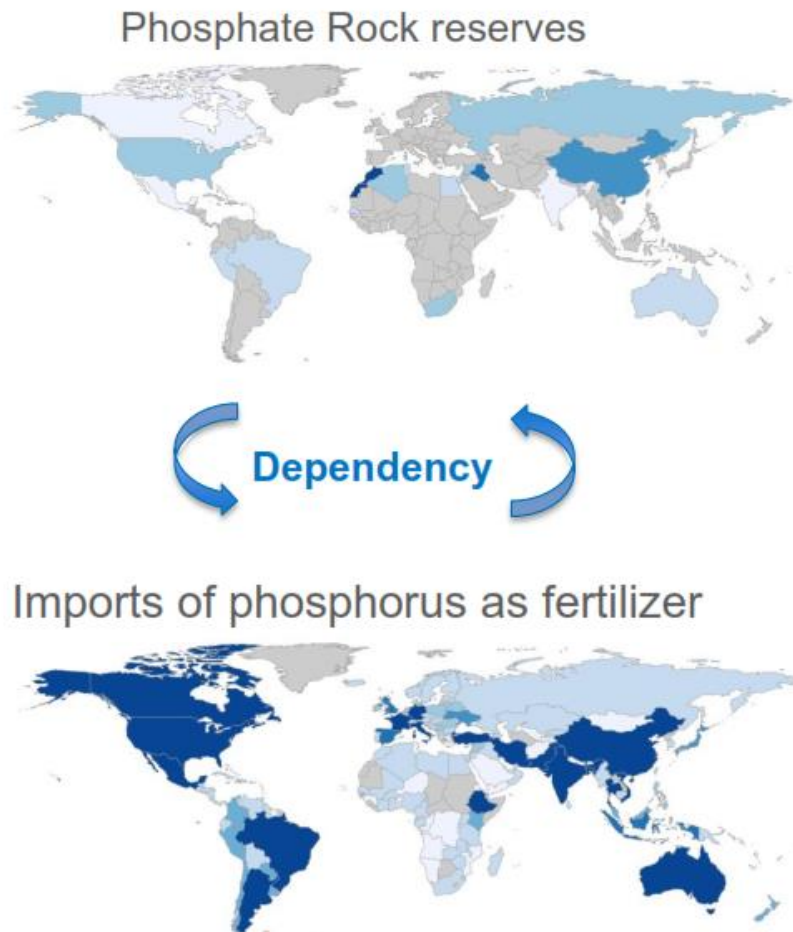


Figure 1 Countries with phosphorus reserves and countries that are importers of phosphate rocks(De Ridder, Jong, Polchar, & Lingemann, 2012)



Figure 2 Phosphorus Cycle(UNEP Year Book 2011)

An individual discharges up to 2g of phosphorus into the wastewater each day. This makes removal and recovery of phosphorus in domestic wastewater important. The inorganics coming from effluent of conventional anaerobic digester treating black water contains nutrients such as ammonia and phosphate. These nutrients could be removed using an algae-bacteria consortium in photo-sequencing batch reactors(PSBR). PSBRs use the photo oxygenation by algae for biological nitrogen removal(BNR), via nitrification and denitrification. A consortium of algae and bacteria in well settling flocs may remove both nitrogen and phosphorus. This combines the advantage of high rate algae ponds and conventional activated sludge processes. Phosphorus removal in PSBR can be achieved with three processes:

1. Biological removal via uptake for algae growth.
2. Chemical precipitation in form of calcium phosphate and magnesium ammonium phosphate(MAP)
3. Enhanced biological phosphorus removal (EBPR) which is done by Phosphorus accumulating organisms (PAOs)

The removal of phosphate is generally carried out by chemical addition because of its simplicity of operation and ease of implementation. In chemical precipitation under the conditions of high pH and low bicarbonate alkalinity, the inorganic orthophosphate can very effectively be precipitated with Ca^{2+} ions as calcium phosphate. Low bicarbonate alkalinity is also the primary requirement for the formation of calcium phosphate. This dependency of the rate of calcium phosphate production from low alkalinity was reported by Song, et al. (2002) .

In PSBR, photo oxygenation via photosynthesis by algae consumes inorganic carbon therefore reduces alkalinity and increases the pH. Also during the biological nitrogen removal the nitrifiers consume inorganic carbon and release hydrogen ion in effect decreasing the alkalinity, but reducing the pH. The processes carried out by algae bacteria consortium in PSBR are potentially ideal for chemical removal of phosphorus from the reactor. The phosphorus removal/recovery is made possible in PSBR by biologically achieving conditions which are high pH and low alkalinity .Since the calcium concentration is limited therefore dosing calcium chloride in the reactor is required to precipitate calcium phosphate.

Illuminating the PSBR with LED as artificial light source by exploiting the high spectrum absorbance of chlorophyll to red light may help in increasing the energy efficiency of oxygenating the reactor which is higher as compared to blowers that are used in conventional SBR processes. LED lighting also helps in reducing the footprint area of the photo bioreactors as it can be submerged to increase the light penetration when the water depth is high.

1.2. Statement of the problem

Phosphorus removal and recovery is one of the focus area in the domestic wastewater treatment. The effluent of the conventional anaerobic digester treating domestic wastewater consists mostly the nutrients such as nitrogen and phosphorus. The COD being consumed in the anaerobic digester is released in the form of carbon dioxide and methane. The carbon dioxide being released gets dissolved and increases the bicarbonate alkalinity of wastewater. PSBR using algae bacteria consortiums serve as an effective tertiary treatment for the effluent from the anaerobic digester. The biological nitrogen removal occurs in PSBR mostly through nitrification, which decreases the pH and consume the bicarbonates by utilizing the oxygen from the photosynthesis. The algae photosynthesis in light phase consumes bicarbonates which in effect raise the pH. When ammonium is removed and no nitrification occurs, then pH increase can be expected due to algae photosynthesis. The research aims to remove/recover phosphorus effectivity from wastewater using the algae bacteria consortiums and study whether the increase in pH damages the nitrification capacity of the biomass.

1.3. Objectives

1.3.1. Overall Objective

To determine the phosphorus removal efficiency via biological and chemically induced precipitation of calcium phosphate at pH values in range of 7.3 to 9 and its effect on nitrification in photo sequencing batch reactor

1.3.2. Specific Objectives

- To determine rate of alkalinity consumption occurring in algae-bacteria consortium
- To determine ammonium removal rate and to determine the effect on nitrification rates of different pH end points.
- To determine phosphorus removal efficiency via calcium phosphorus precipitation at slightly alkaline pH in PSBR at different pH set point.
- To determine effect of solution condition on the precipitation of calcium phosphate in PSBR

1.4. Scope

The experiments were conducted at Asian Institute of Technology (AIT), Phathumthani, Thailand in the laboratory under controlled conditions. The inoculums of algae were obtained from AIT's waste stabilizing ponds and an inoculum of nitrifier was obtained from the sludge of AIT's Sewage Treatment Plant. Synthetic wastewater was modified BG-11 medium having phosphorus, ammonia and bicarbonate alkalinity similar to effluent of anaerobically digested municipal wastewater.

The PSBR was operational at different pH set points to access the effect on chemical phosphorus removal. The PSBR will be illuminated with artificial light (LED) for 11hr.

1.5. Limitations

- Phosphorus concentration is considered to limiting parameter in calcium phosphate precipitation
- Mass balance of phosphorus cannot be done due to the varying luxury uptake of algae
- The synthetic wastewater mimics only the approximate concentration of nutrients which are nitrogen and phosphorus in the effluent of anaerobic reactor, the COD has been kept constant.
- Removal rate of Phosphorus cannot be found since it is dependent on particle size of calcium phosphate

1.6. Assumptions

- There is no suspended solids in the effluent of an anaerobic digester
- Nutrients are present only in the form of phosphates(PO_4^{3-}) and ammonia(NH_4^+)
- The pH of effluent of anaerobic digester is 7.5-8
- Phosphorus removal is not carried out by PAOs

CHAPTER 2. LITERATURE REVIEW

2.1. Algal-Bacterial symbiotic photo bioreactor

The ability of microalgae to take up nutrients from water make them suitable for wastewater treatment (Benemann, 2013). In photo bioreactor single species of algae is grown, whereas in algal system for wastewater treatment contain a consortia of different microbes as wastewater itself contain large variety of different microbes (Li et al., 2014) where a synergetic activity is observed which has potential to improve organic carbon, N and P removal.

One cooperation which has been documented between algae bacteria consortium is related to gas exchange. Oxygen produced by algae during photosynthesis is used by bacteria to breakdown organic compound to CO_2 , which algae can then use to produce further oxygen. Microalgae is known to get important nutrient such as B12 (Croft, Lawrence, Raux-Deery, Warren, & Smith, 2005) from bacteria. Amin, Parker, & Armbrust (2012) has described inter kingdom signaling between algae and bacteria which can help understand type of bacteria and algae that are present locally. There are reports suggesting genetic information being exchanged between algae and bacteria via horizontal gene transfer (Brembu et al., 2014).

In an algae bacteria consortium, the pollutant load removal is achieved basically by algal assimilation, biological processes mainly nitrification (by autotrophs) and denitrification (by heterotrophs), ammonia volatilization and phosphorus precipitation. Stripping phenomenon such ammonia volatilization and phosphorus precipitation are achieved by high pH induced through photosynthetic algae growth. The nutrient uptake efficiency of algae bacteria consortium depends on complex interaction between different physio chemical factors such as pH, light intensity, photo period, temperature and bio flocculation. Photoperiod greatly impacts removal of nutrients, biomass produced and alters the algae bacteria population dynamics. Composition of algae and bacteria community has a large effect both on treatment capability of photo bioreactor and biomass production (Green, Bernstone, Lundquist, & Oswald, 1996).

Full nitrification was observed in algae bacterial consortium without mechanical aeration by Karya et.al, (2013) using synthetic wastewater ($50 \text{ mg NH}_4^+ \text{-N L}^{-1}$). Wang, et.al (2015) also reported $95 \pm 6\%$ NH_4^+ removal and $93 \pm 3\%$ total nitrogen removal from centrate of anaerobically digested swine manure having NH_4^+ loading rate of $76 \pm 14 \text{ mg L}^{-1} \text{ d}^{-1}$

2.1.1. Algal communities

Algae usually exist in natural environment such as lakes and seas in large communities with many different species. These communities change over season and year depending on the environmental condition (Willén, 1987). However photo bioreactor have been built to grow monoculture with *Chlorella* and *Scenedesmus* being the most commonly used genera. This is done so that the selected strains can be maintained and controlled for their characteristics and ideal environmental parameter (Wu et al., 2014). The algae strains in wastewater are selected based on their ability to grow in specific waste or reduce the level of toxic compound present (Muñoz & Guieysse, 2006). Wu et al. (2014) concluded that photo autotrophic unicellular green microalgae are tolerant to many wastewater condition and therefore most commonly used based on his review of microalgae species in wastewater treatment. Wu et al. (2014) also observed that some microalgae species such as *Bitryococcus braunii*, *C. vulgaris* and *S. obliquus* may grow both phototropic and mixotrophically depending on organic matter in different type of wastewater. Photo bioreactor have been inoculated with these stains in many studies (Escapa, Coimbra, Paniagua, García, & Otero, 2015; González, Marciniak, Villaverde, García-Encina, & Muñoz, 2008; Park, Seo, & Kwon, 2012; Posadas et al., 2014). Some authors have tried mixture of different algae species such as mixture of *Schdesmus* and *Desmodemus* sp (Carney et al., 2014) in addition to using monoculture. In mixed culture, the system can be more adequate to the environmental condition. Mixed consortium of algae in photo bioreactor have more resilience to different conditions than pure culture (Muñoz & Guieysse, 2006). The biomass produced could be useful for biodiesel (Rawat, Ranjith Kumar, Mutanda, & Bux, 2013) or biogas (Olguín, 2012) to effect energy requirement. (Chaiwong, 2016) in his experimental study used the inoculum from AIT pond and cultured algae using red led light in PBR using cess pit effluent as wastewater observed *Chlorella* sp.(95.6%), *Synechocystis* sp.(2.3%), *Phormidium* sp.(1.8%) and *Monoraphidium* sp.(0.1%).

2.1.2. Bacterial Communities

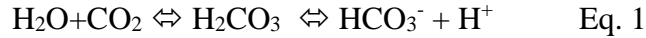
The term “phycosphere” is used to describe the area around micro algae cells or colonies “in which bacteria growth is simulated by extra cellular product of algae” (Bell & Mitchell, 1972). A photo bioreactor using wastewater as a growth medium is bound to contain a rich microbial diversity when no costly sterilization is done.

Carney et al. (2014) described the microbiome of a prototype photo bioreactor treating wastewater where bacteria from proteobacteria and bacteroideter were dominant. Gamma proteobacteria such as *shewanella* and *Rheinheimera* comprised the majority of bacteria, immediately after inoculation. However alpha proteobacteria from genus *Rhizobium* were dominant after two weeks. Krohn-Molt et al., (2013) studied the micro algae *C. vulgaris* and *S. obliquus* association with bacterial biofilm in photo bioreactor system using a liquid medium containing fertilizer supplement with KNO₃. Association of several bacteria from phyla Bacteroides and Proteobacteria with marine macroalgae (Chlorophyta variety) are known (Goecke, Labes, Wiese, & Imhoff, 2010). Bacteria are used as inoculant in agriculture to promote plant growth. Similar principal could be applied to microalgae in photo bioreactor. Gonzalez & Bashan (2000) and de-Bashan, Hernandez, Morey, & Bashan (2004) demonstrated that wastewater

produce higher growth of algae and better nutrient removal when microalgae is grown together with *Azospirillum brasilense* compared to microalgae without *A.brasilen*

2.2. Carbonate Alkalinity

The carbon dioxide been generated in anaerobic digester gets partially dissolved in the effluent of the reactor to form carbonic acid. The carbonic acid rapidly dissociates to form bicarbonates ion and hydrogen ions as shown in the following reaction.



The carbonate system is defined by concentration of five species which are CO_2 , HCO_3^- , CO_3^{2-} , H^+ and OH^- . Carbonate are weak acid and bases which are characterized by the fact that they dissociate only partially in the pH range 0-14. This makes carbonate system a good buffer agent. The dissolved carbonate species play a significant role in stabilizing the pH of the water bodies. The pH stability parameter is evaluated by buffer index which is defined as amount of strong base or acid required to produce a unit change in the pH.

$$B_i = \frac{dC_b}{dpH} = \frac{dC_a}{dpH}$$

Where,

B_i =Buffer index

C_b =No of moles of strong base

C_a =No of moles of strong acid

The carbonate system has two dissociations constant since it is a diprotic weak acid and base system. The Figure 3 shows the buffer index as function of pH with two dissociation constant $\text{pK}_1=6.3$ and $\text{pK}_2=10.3$ at carbonate concentration of 10mmol/l. As it can be seen pH stability (buffer index) is maximum when pH is equal to pK_a .

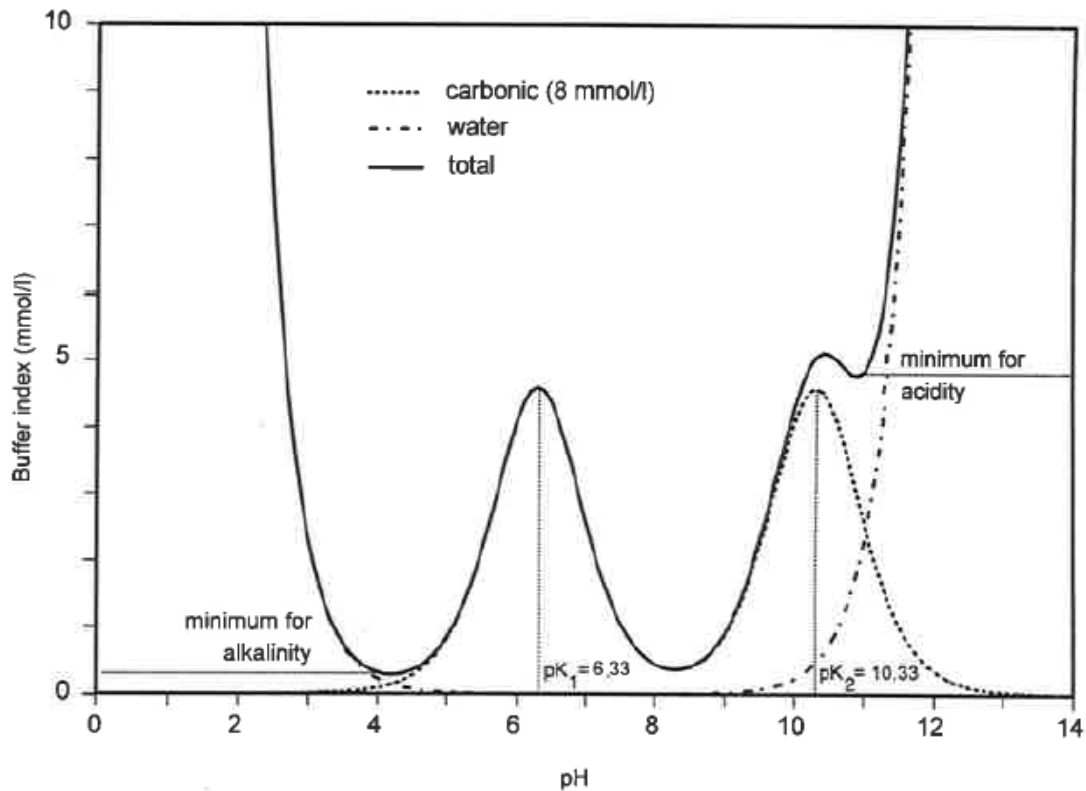


Figure 3 Buffer index as a function of pH for a solution of the carbonate system (Conc: 10 mmol/l) in water

The carbonate system can be defined completely by five equations in which the first three are dissociation equations:

- a) Dissociation constant K_w (Harned and Hamer 1933)
 $K_w = [H^+][OH^-]$
 $pK_w = 4787.3/T + 7.132 \log T + 0.0103T - 22.801$
- b) Dissociation constant K_1 (Harned and Davis 1943)
 $K_1 = [HCO_3^-][H^+]/[CO_2]$
 $pK_1 = 17.052/T + 215.21 \log T - 0.12675T - 545.56$
- c) Dissociation constant K_2 (Harned and Scholes 1943)
 $K_2 = [CO_3^{2-}][H^+]/[HCO_3^-]$
 $pK_2 = 2902.39/T + 0.0239T - 6.498$
- d) Determination of pH
- e) Determination of alkalinity (Loewenthal and Marais 1986)
 $Alk = 2[CO_3^{2-}] + [HCO_3^-] + [OH^-] - [H^+]$

$$pH = -\log[H^+]$$

2.2.1. Alkalinity

Alkalinity is the quantitative capacity of the solution to neutralize acid. To determine alkalinity the solution is considered to be a mixture of CO_2 and a (hypothetical) strong base. Alkalinity is equal to strong base which can be determined by titrating water with strong acid to neutralize strong base. The alkalinity is expressed as concentration of a strong acid i.e. its unit is given in eq l^{-1} or meq l^{-1} .

The total alkalinity is bicarbonate, carbonate and hydroxide alkalinity. The ion concentration is given in molar concentration, the equation below takes into account the charge differences and is adequate to take into account various sources of alkalinity.

$$\text{TA} = (\text{HCO}_3^-) + 2(\text{CO}_3^{2-}) + (\text{OH}^-)$$

Total Alkalinity is expressed as moles/l CaCO_3

The equations necessary for calculation of bicarbonate, carbonate and hydroxide alkalinities as CaCO_3 mg/L are:

$$\text{Bicarbonate alkalinity (CaCO}_3 \text{ mg/L)} = 50,000 \left(\frac{2\text{TA} - 10^{-14+\text{pH}}}{1 + 2K_2 10^{\text{pH}}} \right)$$

$$\text{Carbonate alkalinity (CaCO}_3 \text{ mg/L)} = 100,000 (K_2(\text{HCO}_3^-)(10^{\text{pH}}))$$

$$\text{Hydroxide alkalinity (CaCO}_3 \text{ mg/L)} = 50,000 (10^{-14+\text{pH}})$$

Where,

K_2 is the dissociation constant of hydrogen carbonate

TA is total alkalinity

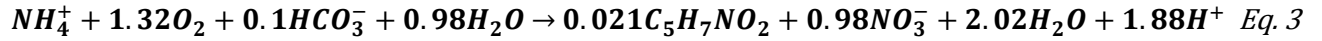
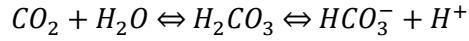
When the pH is between 6.5 and 7.5, the ionic species of water dissociation and the carbonate concentration are much smaller than the bicarbonate concentration therefore the alkalinity due to carbonate system can be taken as concentration of bicarbonates and can be called as bicarbonate alkalinity.

$$\text{Alk} = [\text{HCO}_3^-]/2 \text{ when } 6.5 < \text{pH} < 7.5$$

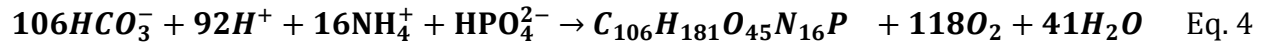
The anaerobic digestion of organic matter gives byproducts carbon dioxide and methane gas. When the saturation concentrations of carbon dioxide and methane in liquid phase are exceeded the biogas is produced. The partial pressure of CO_2 is much smaller than partial pressure of methane. In anaerobic digestion, methane and carbon dioxide is produced in approximately equimolar concentration therefore major part of the CO_2 produced remains in the solution. Apart from alkalinity generated by CO_2 , alkalinity is increased by ammonification and VFA removal.

The consumption of alkalinity occurs in PSBR by two processes which are nitrification and photosynthesis of algae

The oxidation of ammonia through nitrification is a process that consumes bicarbonate thus reducing alkalinity. Also pH decrease is observed as the process releases protons. The stoichiometry of the nitrification reaction is given below (Mara, 2003)



The consumption of bicarbonate alkalinity occurs during the algae photosynthesis. A pH increase is observed as it consumes protons. The stoichiometry of photosynthesis reaction (Mara, 2003) is given below:



2.3. Calcium phosphate precipitation

Formation of calcium phosphate is a difficult phenomenon occurring in different phases under different physical and chemical environment in saturated solution. The different of calcium phosphate (Barat et.al, 2011) are shown in

Table 1 Calcium phosphate phases

Phase	Composition	Molar ratio Ca/p
Brushite(DCPD)	$\text{CaHPO}_4 \cdot 2\text{H}_2\text{O}$	1
Monetite(DCPA)	CaHPO_4	1
Octa calcium phosphate (OCP)	$\text{Ca}_8\text{H}(\text{PO}_4)_6 \cdot 2.5\text{H}_2\text{O}$	1.33
Amorphous calcium phosphate(ACP)	$\text{Ca}_4\text{H}(\text{PO}_4)_2 \cdot x\text{H}_2\text{O}$	1.5
Tri calcium phosphate(TCP)	$\text{Ca}_3(\text{PO}_4)_2$	1.5
Hydroxyapatite(HAP)	$\text{Ca}_5(\text{PO}_4)_3\text{OH}$	1.67

Among all the different kind of calcium phosphate precipitation HAP is the most thermodynamically stable one. The thermodynamic driving force for a chemical reaction is Gibbs free energy which is given by:

$$\Delta G = - \frac{2.303.R.T.SI}{n} \quad \text{Eq. 5}$$

Where R=Ideal gas constant

n=no of moles

T=Temperature

SI=Saturation Index

The saturation Index of a solution is a good indicator for thermodynamic force for precipitation is defined by

$$SI = \log(S) \quad \text{Eq. 6}$$

where S=Super saturation

Super saturation is a measure of the deviation of a dissolved salt from its equilibrium value, for a solution departing from equilibrium is bound to return to this state by the precipitation of the excess solute. The super saturation (S) of system given by:

$$S = \frac{\text{Ionic activity product (IP) in solution}}{\text{solubility product (Ksp)}}$$

where Ionic activity product of HAP (Y Song, et. al, 2002) can be defined as

$$IP_{HAP} = (C_{Ca^{2+}} \cdot f_2)^5 \cdot (C_{PO_4^{3-}} \cdot f_3)^3 \cdot (C_{OH^-} \cdot f_1) - (K_w / [H^+]) f_1 \quad \text{Eq. 7}$$

Where f_i denotes the activity coefficient of i valent ion and K_w refer to the ionic product of water.

When $SI=0$ then $\Delta G=0$, it means the solution is in equilibrium, calcium phosphate precipitation occurs. The solution is oversaturated when $\Delta G<0$ and $SI>0$. However, spontaneous precipitation is not observed when super saturation is achieved since there is a zone between under saturated and spontaneous precipitation zone which is metastable zone. In metastable zone, the solution is supersaturated but no precipitation is occurring over a relatively long period (Stumm & Morgan, 1996). At critical super saturation precipitation occurs which is a boundary between metastable zone and spontaneous precipitation zone (Joko, 1985).

The saturation index of HAP can be evaluated by specifying

$$SI = \log(S) \quad \text{Eq. 6 as}$$

$$\begin{aligned} SI &= \log(IP) - \log(K_{sp}) \\ &= \log[(C_{Ca^{2+}} \cdot f_2)^5 \cdot (C_{PO_4^{3-}} \cdot f_3)^3 \cdot (C_{OH^-} \cdot f_1)] - \log K_{sp} \\ &= 5\log(C_{Ca^{2+}}) + 3\log(C_{PO_4^{3-}}) + \log(C_{OH^-}) + \log(f_2^5 f_3^3 f_1) - \log K_{sp} \end{aligned}$$

This shows that saturation index is related to calcium, phosphorus, pH and solution background which is the ionic strength. Song, Hahn, & Hoffmann (2002) reported functional relationship between calcium concentration and pH with a high correlation coefficient for different phosphorus concentration.

The precipitation reaction model based on the chemical equilibrium and ion concentration, supposes a quick solid formation once exceed saturation index. But this hypothesis over estimates considerably the precipitation. Since there is a zone between under saturated and spontaneous precipitation zone which is metastable zone. In metastable zone, the solution is supersaturated but no precipitation is occurring over a relatively long period (Stumm & Morgan, 1996). At critical supersaturation precipitation occurs which is a boundary between metastable zone and spontaneous precipitation zone (Joko, 1985). Therefore the precipitation and dissolution process of the solid components have to be modelled with kinetic expression.

The kinetics of the processes have been found to be surface controlled based on the theory of Koutsoukos. et al,(1979). Koutsoukos(1979) by addition of well characterized seed crystals to the solution studied the rate of crystallization by following concentration changes as function of time expressed by the equation of the form:

$$\frac{d[M_{v+}, A_{v-}]}{dt} = -k. s. [([M^{m+}]_t^{v+} [A^{a+}]_t^{v-})^{1/v} - ([M^{m+}]_0^{v+} [A^{a+}]_0^{v-})^{1/v}] \quad \text{Eq. 8}$$

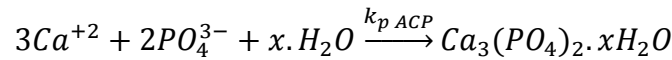
where $[M^{m+}]_t, [A^{a-}]_t$ and $[M^{m+}]_0, [A^{a-}]_0$ are the concentration of crystal lattice ion in solution at time t and at equilibrium respectively

k is the precipitation rate constant

s is proportional to the number of available growth site on the added seed material

n =constant, typically 2

Based on the theory of Koutsoukos et al., (1979), Barat et al., (2011) proposed kinetic expression for the precipitation of reaction for amorphous calcium phosphorus as shown in equation



$$\frac{dX_{ACP}}{dt} = k_{p ACP} \cdot \frac{K_{ACP1}}{K_{ACP1} + \frac{X_{ACP}}{X_{TSS}}} \cdot \left([Ca^{2+}]^{3/5} [PO_4^{3-}]^{2/5} - \left(\frac{K_{SP ACP}}{\gamma_d^3 \cdot \gamma_t^2} \right)^{1/5} \right)^2 \cdot \frac{1 + \text{sign}(SI_{ACP})}{2}$$

The amorphous calcium phosphate dissolution is shown in equation and kinetics in equation

$$Ca_3(PO_4)_2 \cdot xH_2O \xrightarrow{k_d ACP} 3Ca^{+2} + 2PO_4^{3-} + x.H_2O$$

$$\frac{dX_{ACP}}{dt} = k_{d ACP} \cdot \frac{X_{ACP1}}{K_{ACP2} + X_{ACP}} \cdot \left([Ca^{2+}]^{3/5} [PO_4^{3-}]^{2/5} - \left(\frac{K_{SP ACP}}{\gamma_d^3 \cdot \gamma_t^2} \right)^{1/5} \right)^2 \cdot \frac{1 - \text{sign}(SI_{ACP})}{2}$$

where

X_{ACP} is concentration (mol/l)

X_{TSS} is total suspended solids concentration ($g\ m^{-3}$),

$[Ca^{2+}]$, $[PO_4^{3-}]$ are orthophosphate ions concentration ($mol\ l^{-1}$)

$k_{p ACP}$ and $k_{d ACP}$ are ACP precipitation and dissolution constant rate respectively ($l\ mol^{-1}\ d^{-1}$)

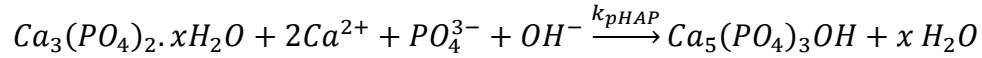
$K_{SP ACP}$ is the ACP solubility product ($mol\ l^{-1}$)⁵

γ_d and γ_t are the activity coefficient of diprotic and triprotic species

K_{ACP1} is the ACP precipitation hyperbolic inhibition constant ($mol\ l^{-1}$)

K_{ACP2} is the ACP dissolution hyperbolic inhibition constant ($mol\ l^{-1}$)

The crystallization of the most stable phase which is HAP is show in equation



This clearly indicates that kinetic of ACP which is precursor to HAP is a surface controlled process (Hartley et. al, 1997) observed that precipitation occur where high pH gradient exist, normally found near the algae cell because during the photosynthesis pH is increased via photosynthesis of algae.

2.3.1. Effect of Carbonate in calcium phosphate precipitation

High carbonate concentration was conjectured as the main problem for the crystallization of calcium phosphate in a pilot wastewater treatment plant in Darmstadt-Eberstadt Sewage Treatment Plant, Germany (Driver et.al, 1999).

The formation of calcite is considered to be the main reason since it has more saturation index than calcium phosphate when carbonate concentration is high. The studies conducted by Van der Weijden, et al (1997) and Lin & Singer, (2005) have demonstrated that for a same degree of supersaturation the calcite precipitation increased with increase in carbonate anion /calcium cation ratio of the solution. This finding contradicts the fact that supersaturation is the only parameter of precipitation kinematic.

John F. Ferguson, (1973) demonstrated that it is possible to achieve phosphate residual of below 2 mg/l by calcium phosphate precipitation at pH below 9. It has been observed by Ferguson that a period of very slow precipitation which is an induction period is followed by rapid precipitation and then further slow precipitation as the reactant (phosphate) approaches equilibrium value, c_o .

During the induction period, the reactant concentration change and then a crystal growth period occur where reactant concentration falls exponentially towards an equilibrium level. The rate of crystal growth depends on two variable which are the availability of surface area and concentration of limiting reactant. This can be described by the below equation.

$$\frac{\partial c}{\partial t} = -k \cdot s \cdot (c - c_o)^n$$

where

n = order of reaction

s = available crystal surface area

c = concentration of the limiting reactant

c_o = equilibrium concentration, and

t = time from the end of the induction period

John F. Ferguson, (1973) suggested that bicarbonate concentration led to an increase in induction period and therefore subsequent decrease in the removal rate of phosphate. This effect could be empirically incorporated in rate equation as follows.

$$\frac{\partial c}{\partial t} = \frac{-K'}{CO_{3T}} c^n$$

where, $K' = K CO_{3T}$
 CO_{3T} = bicarbonate concentration at temperature T.

Also decrease in calcium phosphate crystallinity was observed by with increasing bicarbonate concentration.

Experimental testing of these prediction was conducted by John F. Ferguson, (1973) in 4 L reactor followed by 1 L capacity settling tank. The reactor was fed with $CaCl_2$, $NaHCO_3$, $NaOH$, Na_2HPO_4 having an initial concentration of carbonate (1.3mM), calcium (2mM), PO_4^{3-} = 0.25mM and $T = 25^\circ C$ was maintained. When the initial pH was maintained at 7.2, 7.8 and 8.1, phosphorus residual concentration of 0.086, 0.061 and 0.053mM was reported. At pH 8 when initial bicarbonate increased from 1.3 to 7mM it resulted in increase in phosphate residual from 0.053 to 0.099mM. An increase in efficiency of phosphate removal was observed when mixing condition was changed from CSTR to plug flow.

Organic matter can greatly decrease rate of calcium carbonate precipitation as observed by Chave & Suess, (1970) in ocean water. A similar retardant effect can be expected for calcium phosphate precipitation having high concentration of organic matter in algae bacteria consortium of PSBR.

The induction period can be circumvented in a batch reactor which is completely mixed as the phosphate removal rate can be increased by increasing mass of precipitate in the reactor. Ferguson also found that large particle formed by agglomeration of many very small crystals. There was no evidence from electron microscopy or x ray diffraction that large crystal are formed. Thus highlighting kinetics of the process are mostly surface controlled. It was also observed by Reddy, (1977) and Grases & March, (1990) that phosphate get adsorbed to the calcite crystal growth site and inhibit calcite precipitation. Thus reducing both rate and extent of calcite precipitation between pH 7 and 9 directing calcium to particulate in calcium phosphate precipitation.

Bruke, (2016) has removed phosphate in wastewater through calcium phosphate precipitation with elevated pH and reduced alkalinity through consumption of bicarbonate/carbonate by autotrophic microorganism in a proprietary system. The proprietary system schematic is shown Figure 4.

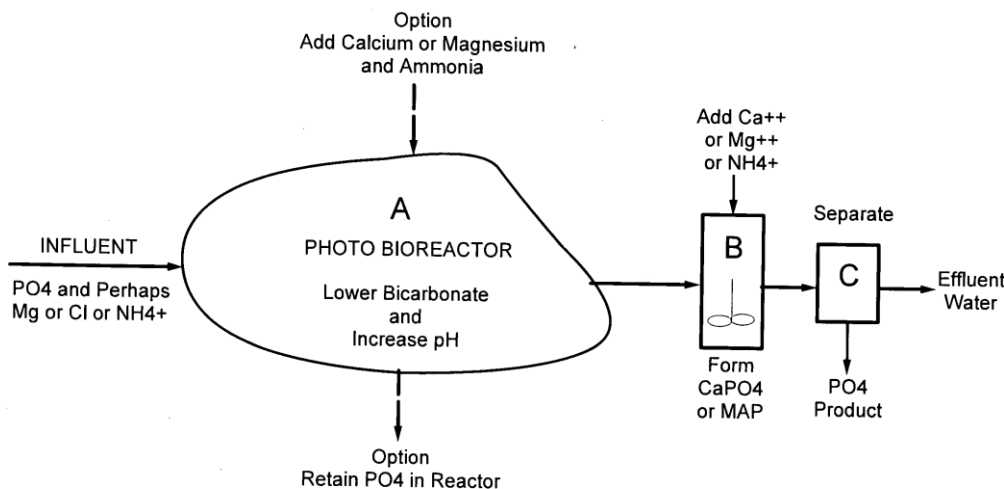


Figure 4 Schematic of phosphorus recovery and removal from liquid scheme

2.4. Phosphorus uptake by algae

Phosphorus has a typical gravimetric share at approximately 0.9% in dry weight of natural microalgae using the Redfield Ratio(C:N:S:P) of 106:16:1.7:1 (gravimetric ratio 41:7.2:1.75:1)(Alfred C. Redfield, 1958).The gravimetric share of P in dry weight can reach up to 1.8% in microalgae fed by swine manure(Kebede-Westhea.et al, 2006) and can even go up to 4% phosphorus in dry weight of algae as reported by (Powell,et.al 2011). This trait of luxury uptake (P retention) can be used for phosphorus removal in wastewater treatment(Boelee, Temmink, Janssen, Buisman, & Wijffels, 2011).

Algae can take up inorganic phosphate (P_i) directly from environment(Atlas, et.al 1976) which depend on both nutritional status (nutritional history) and algae growth rate(Cembella, et.al 1982). Extracellular or cell wall bound phosphatase enzyme decompose more complex bioavailable P compound to inorganic phosphate. The inorganic phosphorus spontaneous diffusion across the lipid layer of algae cell membrane is prevented due to its negative charge. There are two mechanisms by which inorganic phosphorus uptake takes place across the plasmalemma. The first mechanism is the over compensation or “overshoot” (Cembella et al., 1982) which occurs when pre starved algae cells are exposed to P rich environment. Accumulation of acid soluble polyphosphate occurs which is light dependent and rapid as a result of transfer(Aitchison & Butt, 1973).In the second mechanism, luxury uptake happens when P_i is abundant and no pre starvation is required (Eixler et.al, 2006).Due to unstable P availability luxury uptake evolved as an adaptation of micro algae.

Phosphorus retention in algae cells is in form of polyphosphate and also play a central role in many biological processes as it serve as an internal P storage which cells can use when needed (Rasala & Mayfield, 2015). Phosphorus uptake and storage are energy requiring processes that require sufficient

light to drive photosynthesis under autotrophic conditions. The ATP generated during cyclic electron flow around Photosystem I, provides major source of energy for P_i uptake in photophosphorylation (Cembella, et.al 1982).

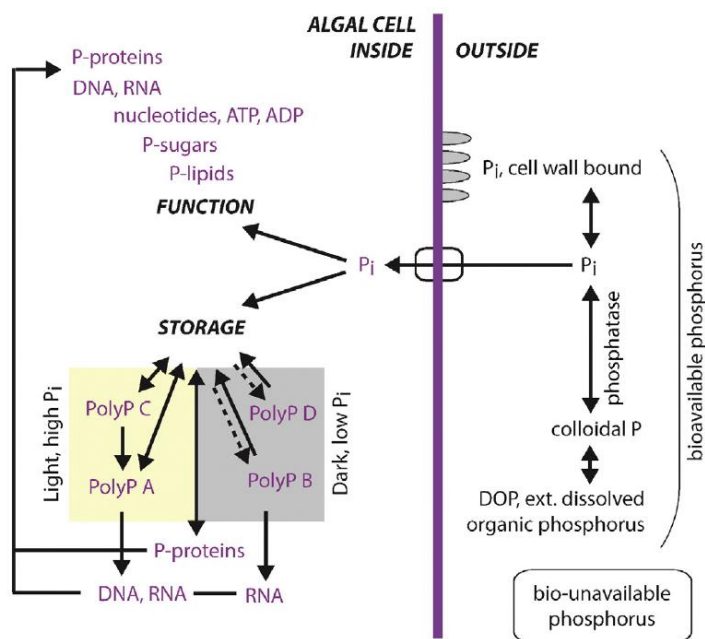


Figure 5 A schematic representation of different P pools and fluxes inside and outside of an algae cell (Solovchenko, et.al , 2016)

Miyachi (Miyachi, et.al 1964; Miyachi & Miyachi, 1961) have differentiated polyphosphates in at least four fractions in algal cells which are A, B, C and D. The acid soluble polyphosphate fractions are A and C that are generated when light and P_i are abundant and can transfer P_i to protein and DNA. The acid insoluble polyphosphate fractions are B and D which cannot be used readily but act as reservoirs in absence of external P_i . Increasing the light intensity induces a decline in the acid-soluble polyphosphate but has no significant effect on acid-insoluble polyphosphate (Brown & Shilton, 2014). This is probably due to rapid division of cells in high irradiance leading to consumption of acid-soluble polyphosphate for biosynthesis of cellular constituents at a higher rate than the polyphosphate replenishment. Under carbon limitation condition photosynthesis is getting hindered even though there is plentiful irradiance. Hence slowed cell growth and cell division is observed but increased polyphosphate content per cell weight occurs suggesting luxury uptake of inorganic phosphate. When energy that cells cannot use for linear photosynthetic energy transfer, it is probably directed to luxury P uptake provided sufficient inorganic phosphate is available (Cembella et.al, 1984).

The general consensus in the literature is that the algae biomass will contain a higher proportion of phosphorus when there are higher concentrations of phosphate in the medium and that this occurs over a wide range of phosphate concentrations (Aitchison & Butt, 1973; Powell et.al , 2006). However, it was demonstrated by Nicola Powell et.al (2009) that the luxury uptake by microalgae consortium is independent of phosphorus concentration in the medium when the concentration is in the range of 5-

30mg L⁻¹ P. They also demonstrated that luxury uptake occurs in form of acid soluble polyphosphate below 15mg L⁻¹ P and above that acid insoluble polyphosphate accumulation occurs.

In the pond environment there are many fluctuating factors making the P transformation process complex and development of luxury P uptake process challenging. However Photo bioreactor allows as a closed system, use of engineered algal strains, energy efficient design supporting intensive cultivation, fine tuning of illumination intensity, mixing rate and temperature based on understanding of luxury uptake by microalgae cells leads to high potential for P removal > 90% ((Posadas et al., 2014; N. Powell et al., 2011).

2.5. Enhanced Biological Phosphorus Removal

Phosphorus takes 1-2% of microorganisms' dry mass in general. It is an essential element of DNA (Deoxyribonucleic acid) that stores genetic information of organisms. It is also an important constituent of ATP (Adenosine-5'-triphosphate) that is an essential component of energy metabolism. Phosphorus exists in wastewater as orthophosphate (PO₄³⁻), polyphosphate, organically bound phosphorus, etc. Around 6 mg of P is removed per g COD in raw wastewater by assimilation mechanisms in typical conventional activated sludge (CAS) process treating municipal wastewater, which corresponds to 25-50 % of total incoming P (Haandel & Lubbe, 2007).

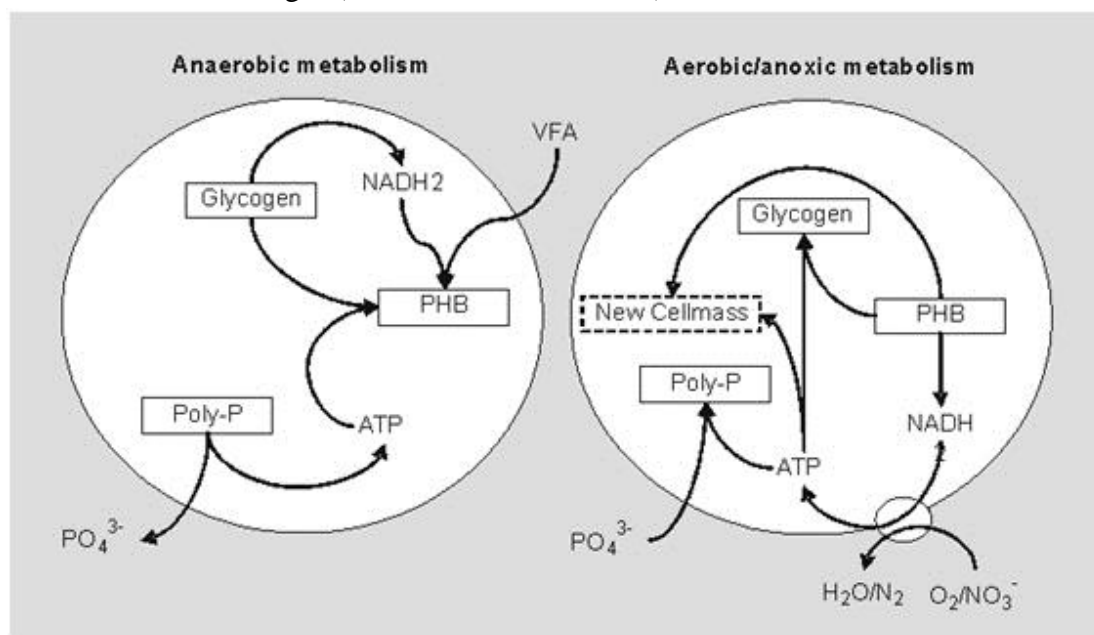


Figure 6 A schematic representation of phosphorus accumulating organism

Additional phosphorus can be removed by enriching phosphorus-accumulating organisms (PAO) in microbial population using enhanced biological phosphorus removal (EBPR) process. PAO is a group of bacteria that can accumulate phosphorus in cell mass at the level much higher than 1-2 %, i.e. up to 38% (Haandel & Lubbe, 2007).

The metabolism of PAO is depicted in Fig. 6. In aerobic condition, PAO uptakes excess phosphorus and stores it as polyphosphate in the cell mass using the energy from the heterotrophic oxidation of organic materials (BOD/COD). If PAO is exposed to anaerobic condition, where little molecular and combined oxygen molecules are available, it obtains energy from the hydrolysis of the accumulated polyphosphate to uptake volatile fatty acids (VFA) as poly-hydroxyalkanoates (PHA) and poly-hydroxybutyrates (PHB). The phosphorus is removed in the EBPR process from wastewater through accumulation in the heterotrophic bacteria present in biomass. EBPR process is technically more complicated than chemical P removal but is the most investigated process due to its widespread application (Martín et al., 2006) especially in agriculture as the sludge can be used as slow release fertilizer. Chemical phosphorus recovery can be combined with EBPR to recover phosphorus in form of struvite after anaerobic digestion of EBPR sludge (Wilfert, et.al, 2015).

2.6. Biological nitrogen removal

Ammonia causes eutrophication in natural water environment and toxic to the aquatic life.

In a nitrogen removal process, the nitrification step in which ammonia in wastewater is oxidized to nitrate by autotrophic nitrifiers is essential, since it is the prerequisite to denitrification in which nitrate produced from nitrification is reduced to N_2 gas, which is ultimately removed from water.

It takes considerable time for the autotrophic nitrifying bacteria to return to their normal state, comparing to heterotrophic organic-oxidizing bacteria.

For biological nitrogen removal sequence of both nitrification and denitrification is necessary (Spanjers, Vanrolleghem, Olsson, & Dold, 1996). The nitrification process is considered to be the most vulnerable in activated sludge process since there are many factors which are interconnected. The nitrifying bacteria are characterized by two distinct properties: slow growth rate and vulnerability to toxic compounds.

Nitrification is comprised of two stages which are ammonia oxidation and nitrite oxidation. The ammonia oxidation is performed by ammonia oxidizing bacteria (AOB) or *Nitrosomas* group which oxidizes NH_4^+ to NO_2^- -N. The nitrite oxidation is performed by the nitrite oxidizing bacteria (NOB) or *Nitrobacter* group that convert NO_2^- -N to NO_3^- -N.

Jiménez, et. al (2011) observed that NOB were strongly affected by low pH (<6.5) but no inhibition was observed for pH range of 7.5-9.95. Whereas observed Jiménez, et. al (2011) that the AOB are very sensitive to pH. Claros et al., (2013), reported that optimal pH for the AOB to function was in the range of 7.4-7.8 and showed high inhibitory effect at high pH.

Under normal conditions, nitrifiers consume more oxygen to oxidize NH_4^+ to NO_2^- or NO_3^- than heterotrophs do to oxidize organics to CO_2 ; thus, 4.2 mg oxygen is required for oxidizing 1 mg NH_4^+ . Oxygen consumption rate (also called oxygen uptake rate (OUR)) has been utilized for directly assessing the activity of nitrifying activated sludge. Practically speaking, oxygen consumption by nitrification processes accounts for approximately 40% of the total oxygen demand in an advanced WWTP (Spanjers et al., 1996). To monitor the two groups in nitrification, decrease of substrate NH_4^+ and increase in NO_3^- . Nitrification monitoring in the algae bacteria consortium using oxygen uptake rate (OUR)

2.7. Artificial illumination

Light energy can be provided with natural or artificial illumination. Sun provides natural illumination but it has light/dark cycle and illuminations vary during the day. By using artificial illumination, the fluctuation in irradiance can be prevented. The photo bioreactor with artificial illumination makes it possible to grow algae strain under well controlled physios-chemical conditions. In horticulture the artificial illumination is been used for the past few years, based on the broad experience three types of lamps are identified which are: florescent tubes, high pressure sodium lamps and LED. The PAR efficiency of the three lamps are shown in table

Table 2 Overview of various light sources (Blanken.W et.al ,2013)

S.No	Lamp Type	PAR efficiency ($\mu\text{mol.ph s}^{-1}\text{W}^{-1}$)
1	Florescent lamp	1.25
2	High pressure sodium vapor lamp(HID)	187
3	LED	1.91

The PAR efficiency of HID and LED is similar, but HID has attained maximum PAR technical efficiency whereas LED is continuously improving. LEDs are therefore preferred choice for artificial illumination. Light emitting diodes (LEDs) since 1980's has significantly enhanced efficiency and have been proposed as a primary light source for bio generative life support system. Their energy efficiency has opened new perspectives for optimizing the energy conversion. LED marks a great advancement over existing indoor agriculture lighting since it allowed control of spectral composition and adjustment of light intensity to simulate the changes of sunlight intensity during the day. Low radiant heat output is produced with high light levels and also maintain useful light output for years.

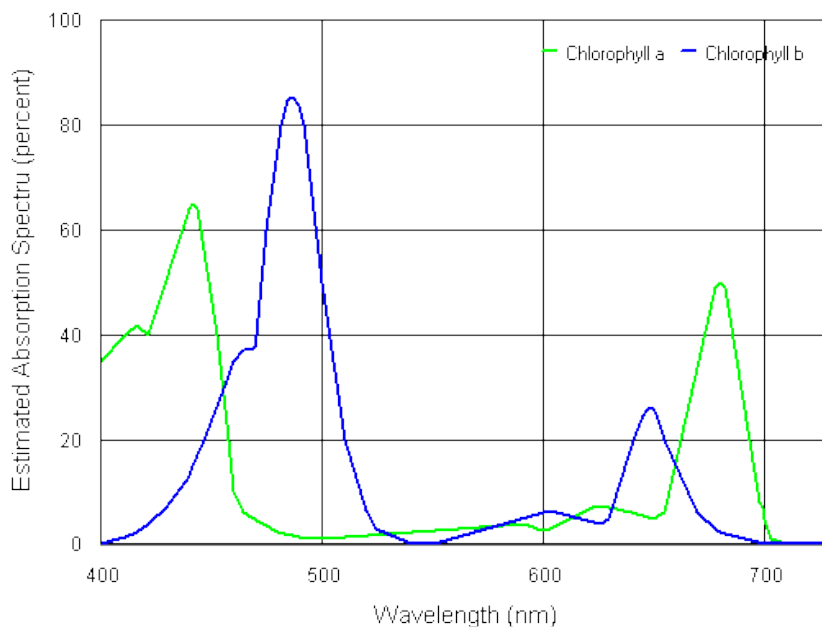


Figure 7 Spectrum absorption efficiency of Chlorophyll a and b(Raven et al. 1976)

In algae photosynthesis pigment play an important role as they capture energy from light. The chlorophylls are the most important and widespread found in all photosynthetic eukaryotes and cyanobacteria. The photosynthetic pigments found in green algae are Chlorophyll a and b, α -, β -, γ -carotenes and several xanthophyll's(Bold and Wynne,1976). The adsorption spectrum of chlorophyll a and b is shown in Figure 7. As it can be seen the algae can employ all photons in the PAR range (400nm to 700nm) with high absorption efficiency in 400-500nm(blue light) and 600-700nm(red light). According to Plank's relation, blue light emits less photon per watt as compare to red light. Therefore utilizing certain spectrum will lead to less energy consumption to oxygenate the photo sequencing reactor where algae bacteria consortium is been used.

CHAPTER

3. METHODOLOGY

3.1. Conceptual Framework

The conceptual framework of study is divided into two phases with two reactors been operated simultaneously. The photo sequencing batch reactor (PSBR) which are Reactor 1 and Reactor 2 were operated with a 12-hour cycle per day and other 12hr the reactors were not stirred and no illumination (Dark Phase). Both the reactors were initially inoculated with the same consortia of algae and bacteria. In Phase 1, both the reactor were kept at controlled 7.3 pH for an entire react time of 11hr. The synthetic wastewater been fed in Phase 1 had the following characteristics: 100 mg N-NH₄⁺/L, 15 mg P-PO₄⁻³/L, 64 mg Ca⁺² /L and 819 mg CaCO₃/L .

In Phase 2, Reactor 1 was kept at 7hr of controlled pH and the 4hr of uncontrolled pH whereas Reactor 2 was kept at controlled pH(7.3) for the entire react stage. This was done to study the effect of increase in pH in the nitrification process. Phase 2 was further sub divided into sub phases based on wastewater characteristics. The wastewater characteristic for phase 2a was: 50 mg N-NH₄⁺/L and 15 mg P-PO₄⁻³/L, 64.2 mg Ca⁺² /L concentration was maintained. The alkalinity was varied to 819, 1219 and 1619 mg CaCO₃/L. For Phase 2b the wastewater characteristics are: 50 mg N-NH₄⁺/L, 15 mg P-PO₄⁻³/L, 1619 mg CaCO₃/L and 13 mg Ca⁺²/L. In Phase 2b both the reactors were dosed with CaCl₂ at the end of the react time. The alkalinity consumption, ammonium removal rate and TSS were studied in all the stages. The phosphorus concentration in the influent and effluent was also analyzed in Phase 2b.

3.2. Preparation of experiment

3.2.1. Synthetic wastewater

The synthetic wastewater mimics the effluent coming from anaerobically digested wastewater and similar to the medium used by (Fredy, 2013) in his study of nitrification in Photo sequencing batch reactor. Ogawa solution was used and applied to the medium as trace element source. The detailed composition of Ogawa solution is shown in Table 4 .

The synthetic wastewater's ammonia, alkalinity and calcium concentration were varied in differed phases for Phase 1, 2a and 2b as shown in **Table 3**. In Phase 2a, ammonia concentration was decreased to 50 mg N-NH₄⁺/L. In Phase 2b, calcium concentration was decreased to 13 mgCa⁺²/L.

Table 3 Synthetic wastewater used as influent for PSBRs during Phase 1 and 2

Compound		Conc.(mg/l)						
		Phase 1	Phase 2a	Phase 2b		Phase 1	Phase 2a	Phase 2b
Sodium Acetate (COD Source)	CH ₃ COONa	95	95	95	<i>COD</i> (mg O ₂ /L)	230	230	230
Citric Acid	C ₆ H ₈ O ₇ .H ₂ O	6.6	6.6	6.6				
Ammonium Chloride	NH ₄ Cl	382	191	191	<i>Ammonia</i> (mg N-NH ₄ ⁺ /L)	100	50	50
Di potassium phosphate	K ₂ HPO ₄	84	84	15	<i>Phosphorus</i> (mg P-PO ₄ ³⁻ /L)	15	15	15
Magnesium Sulphate	MgSO ₄ .7H ₂ O	75	75	7.4	mg Mg ⁺² /L	7.4	7.4	7.4
Calcium Chloride	CaCl ₂ .2H ₂ O	236	236	13	mg Ca ⁺² /L-	64.2	64.2	13
Sodium Bicarbonate	NaHCO ₃	1344	1344	1600	<i>Alkalinity</i> (mg CaCO ₃ /L)	800	800	1600
			2016				1200	
			2688				1600	
Ferrous Sulphate	FeSO ₄ .7H ₂ O	3.4	3.4					
Sodium Carbonate	Na ₂ CO ₃	20	20	20	<i>Alkalinity</i> (mg CaCO ₃ /L)	18.87	18.87	18.87
Sodium Metasilicate Pentahydrate	Na ₂ SiO ₃ .5H ₂ O	44.8	44.8					
Ethylene diamine tetra acetic acid, disodium dihydrate	Na ₂ EDTA.2H ₂ O	1	1					

Table 4 Ogawa Trace element solution

	Compounds	Conc.(mg/l)
1	H ₃ BO ₄	3.5875
2	MnCl ₂ .4H ₂ O	1.810
3	ZnSO ₄ .7H ₂ O	0.220
4	CuSO ₄ .5H ₂ O	0.080
5	(NH ₄) ₆ Mo ₇ O ₂₄ .4H ₂ O	1.288
6	CoCl ₂ .6H ₂ O	0.034
7	NiCl.6H ₂ O	0.043
8	KI	0.180

3.3. Microalgae cultivation

The algae used in the PSBR was cultured by taking inoculum from surface pond water of Asian Institute of Technology, Phatumthani, Thailand which has a mix of different algae species. The algae is initially adapted and enriched with synthetic wastewater (BG-11 Modified) with alkalinity of 800 mg/l as CaCO₃ in PW/WW ratio of 3:7 in 250 ml volumetric flask under LED light illumination of 100 $\mu\text{mol}/\text{m}^2/\text{sec}$ as shown in Figure 3. The culture is stirred with magnetic stirrer and allowed to attain concentration 1200-1000mg TSS/l which took 30 days.



Figure 8 Algae culture using LED lights

3.4. Light Source

Both the PSBRs were illuminated with LED light as artificial light source having wavelength of 600-700nm which is red in color. The LED light source had an intensity of $30\mu\text{mol}/\text{m}^2/\text{sec}$ during Phase 1 and the light intensity was increased to $100\mu\text{mol}/\text{m}^2/\text{sec}$ in Phase 2b during the latter part of the react period using PWM from the Arduino controller connected to it. The illumination intensity and its operation is controlled by raspberry pi (Slave Arduino-Raspberry Pi Master) which apart from data logging also controls the entire operational cycle. The light source of specific wavelength is chosen to promote photosynthesis, producing oxygen with less energy consumption. The illumination of two reactor using red light as source is shown in Figure 9 below.

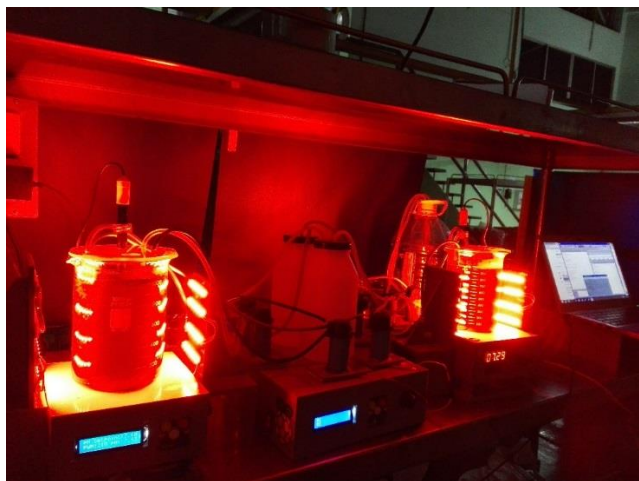


Figure 9 PSBRs illuminated using red led light during react stage

3.5. Lab Scale Photo Sequencing Batch Reactor (PSBR)

A 1 L continuous stirred tank reactor cylindrical in shape made of Plexiglas was used in order to allow light penetration and reach biomass. The reactor received a light intensity of 100 or $33.5\mu\text{mol}/\text{m}^2/\text{sec}$ which was measured using quantum meter (Apogee Instruments Model No.-MQ 200). The light intensity in both the reactors depends on the operating condition for different phases as mentioned in Table 5. The PSBR is equipped with pH controller (Arduino based pH controller) that injects solution of HCl (0.1 N HCl when pH exceeds pH set point).

An automatic feeding system (peristaltic pump) and agitation by magnetic stirrer were also implemented in both the Reactors. The pH controller continuously monitored the pH, temperature and acid addition which were logged using Raspberry Pi. The pH controller (Slave) used in Reactor 1 and Reactor 2 was controlled by Raspberry Pi (Master) which was programmed based on operating condition of different phases. Both photo sequencing batch reactor (PSBR) were operated with one 12hr cycle per day. The operational cycle of Reactor 1 and 2 during different stages is shown in Table 5. The detail operation cycle of Reactor 1 in Phase 2a is shown in Figure 11 and for Reactor 2 is shown in Figure 12.

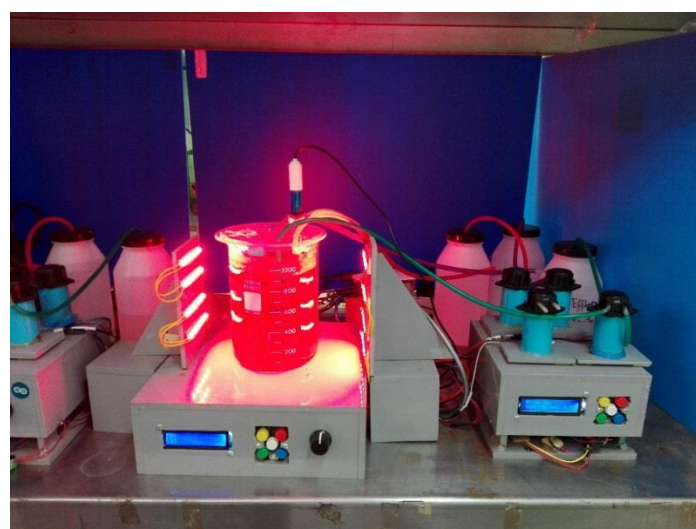
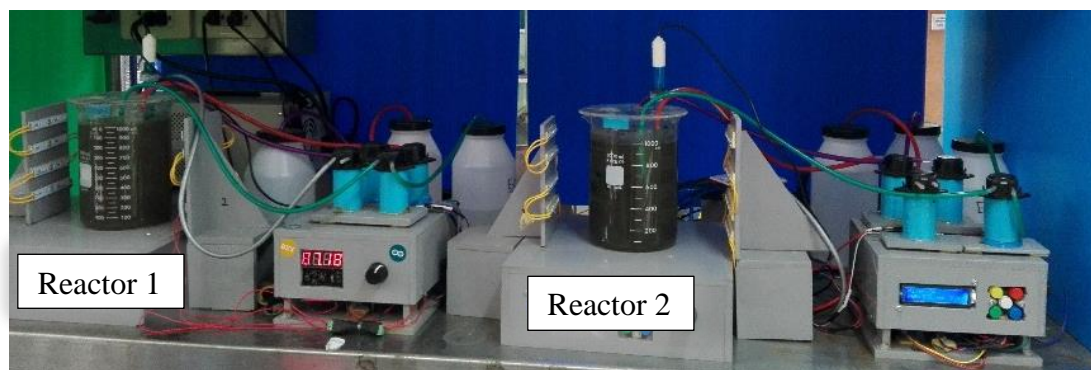
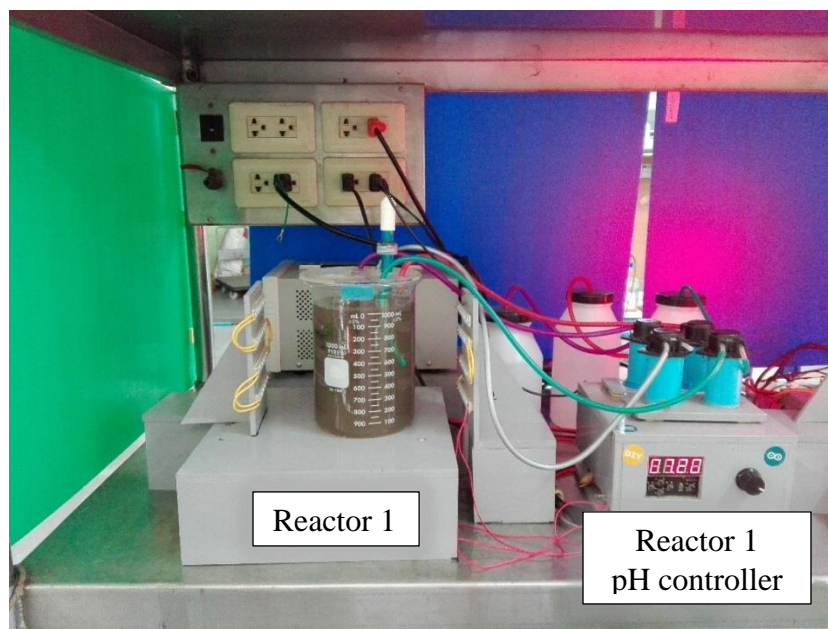


Figure 10 PSBRs Setup during the study period

Table 5 Detail of operational cycle in PSBRs

a. Reactor 1: Phase 1(30 Days)

Duration(hours)	0.25	11	0.5	0.25
Stage:	Feed	React	Settle	Decant
pH Controller	Off	On	Off	Off
	Dark	Light Phase	Dark	

b. Reactor 1: Phase 2a(6 Days)

Duration(hours)	0.25	7	4	0.5	0.25
Stage:	Feed	React		Settle	Decant
pH Controller	Off	On	Off	Off	Off
	Dark	Light Phase		Dark	

c. Reactor 1: Phase 2b(10 Days)

Duration(hours)	0.25	7	4	0.5	0.25
Stage:	Feed	React		Settle	Decant
pH Controller	Off	On	Off	Off	Off
	Dark	Light Phase		Dark	Dark

d. Reactor 2: Phase 1(16 Days) and Phase 2a(6 Days)CaCl₂ Addition

Duration(hours)	0.25	11	0.5	0.25
Stage:	Feed	React	Settle	Decant
pH Controller	Off	On	Off	Off
	Dark	Light Phase	Dark	

e. Reactor 2: Phase 2b(10 Days)

Duration(hours)	0.25	11	0.5	0.25
Stage:	Feed	React	Settle	Decant
pH Controller	Off	On	Off	Off
	Dark	Light Phase	Dark	

CaCl₂ Addition

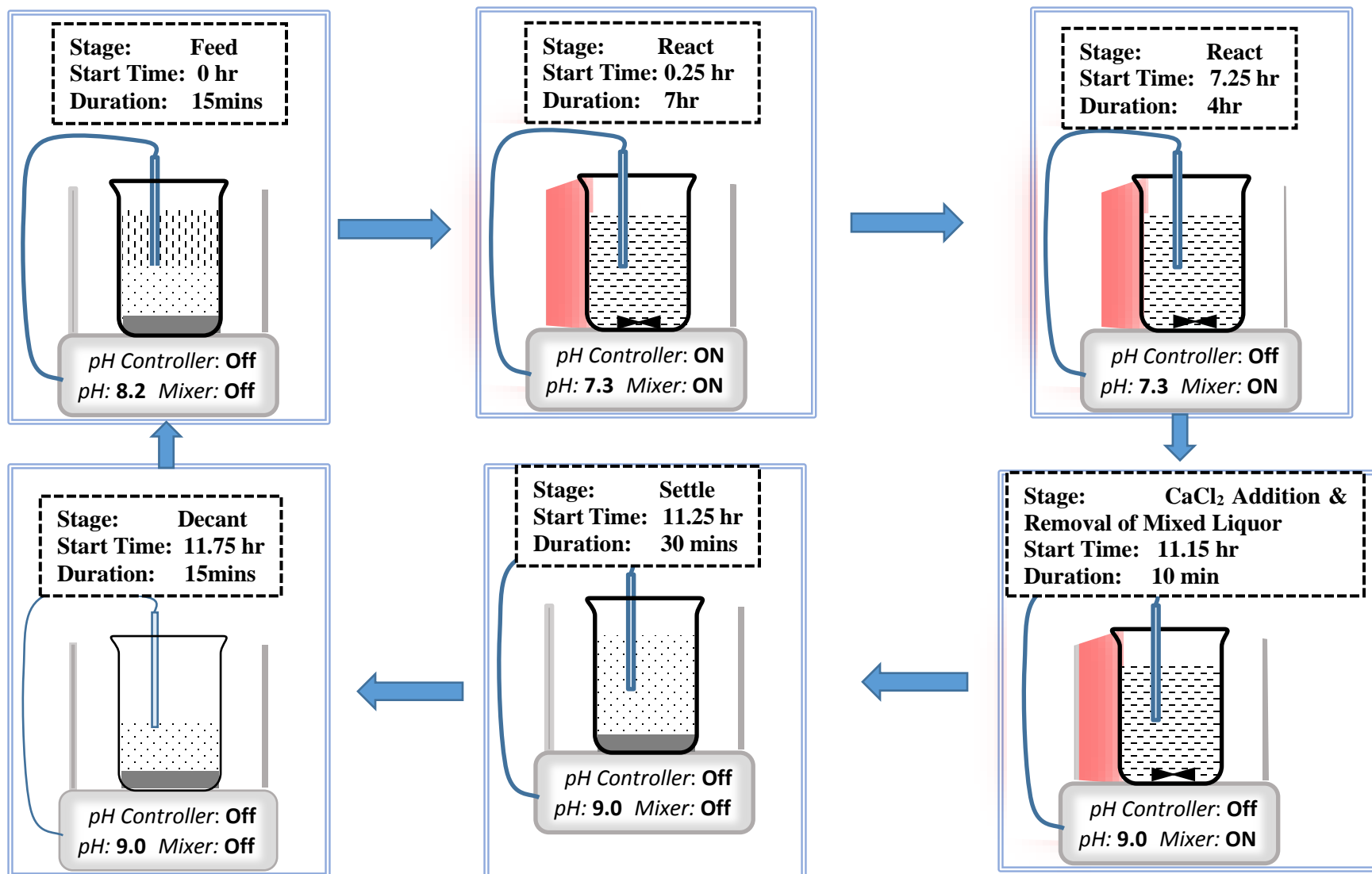


Figure 11 Phase 2b: Operation Cycle of Reactor 1

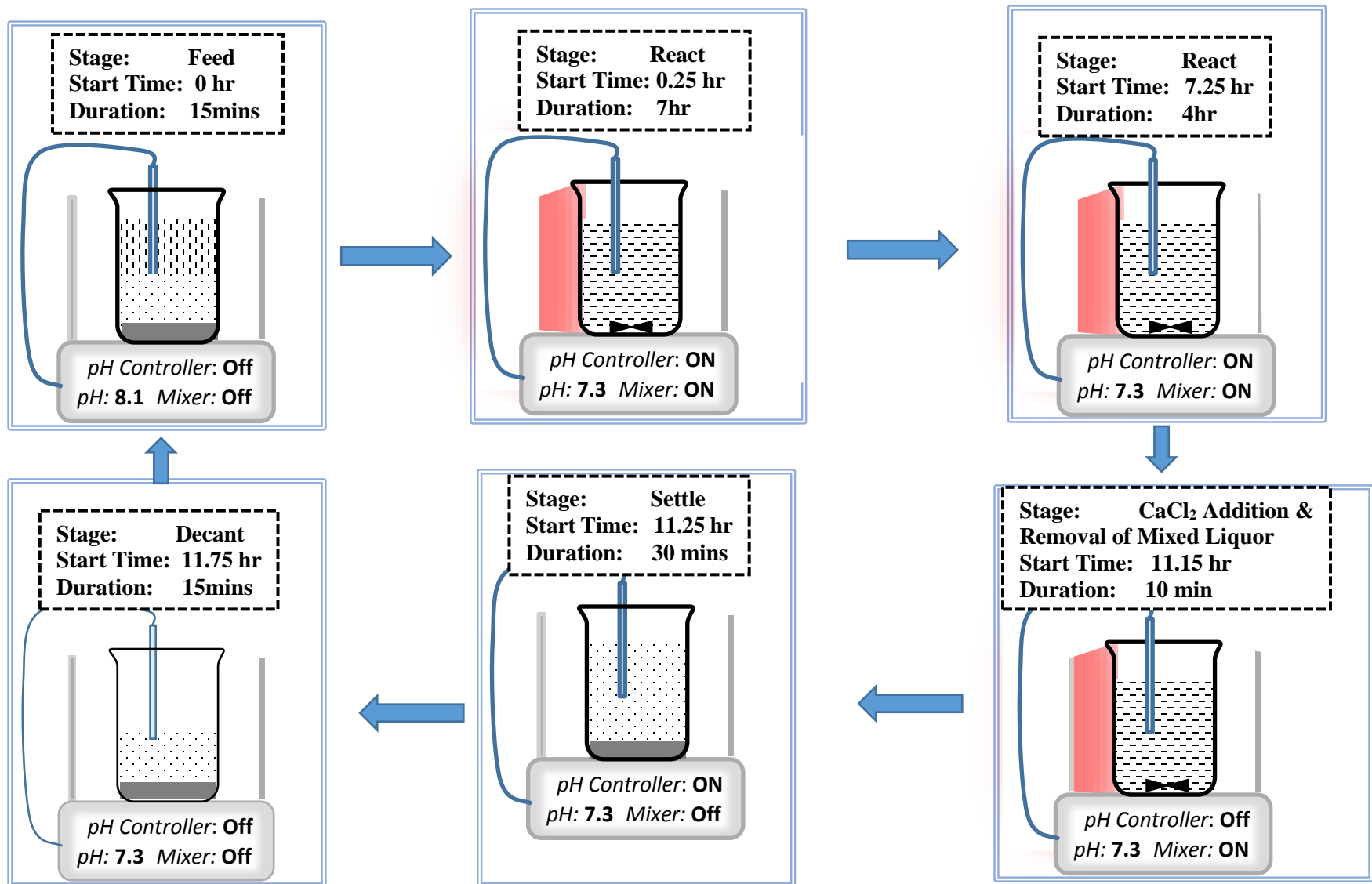


Figure 12 Phase 2b: Operation Cycle of Reactor 2

3.6. Sampling

The two photo sequencing batch (PSBR) reactor were operated for a 12hr cycle per day. Intermittent sampling of both the reactor was carried out at certain defined interval as shown in the Table 6 below.

Table 6 Sampling Schedule during different phases

	Sampling Time(hr)								
	Alkalinity	Ammonia	Phosphorus	Calcium	Nitrate	pH	Temp	DO	Conductivity
	(mg CaCO ₃ /L)	(mg N-NH ₄ ⁺ /L)	(mg P-PO ₄ ³⁻ /L)	(mg Ca ⁺² /L)			(°C)		(mS/cm)
Phase 1	0,3,6,9,12	0,3,6,9, 12	0,12	-		Continuously Monitored		0,3,6 ,9,12	0,12
Phase 2a	0,2,4,6,11	0,2,4,6, 11	0,1,2,3,4,5,6 , 7,8,9,10,11, 12	0,12					
Phase 2b	0,2,4,6,11	0,2,4,6, 11	0,11,11.5	0,12	12				

The analytical methods been used are shown in Table 7 below.

Table 7 Analytical Methods

S No	Parameter	Analytical Method
1	pH	pH meter
2	DO	DO meter
3	Temperature	Temperature sensor
4	NH ₄ ⁺ -N	Distillation Method
5	NO ₃ ⁻ -N	Spectrophotometer
6	HCO ₃ ⁻¹	Titration with H ₂ SO ₄ and indicator bromo cresol green methyl red
7	PO ₄ ⁻³	Ascorbic Acid Test
8	TSS	Dried at 105°C
9	VSS	Dried at 105°C and ignited at 550°C
10	Light Intensity	Quantum Meter
11	Conductivity	Conductivity meter

3.7. Modelling Chemical Speciation

For modeling the chemical speciation, MINTEQA2--a computer program for calculating aqueous geochemical equilibria developed by U.S. Environmental Protection Agency was used. The distribution of an element among different chemical species in a system is called Chemical speciation. It plays an important role in knowing the full speciation of a chemical in order to predict the behavior of the system. It is generally not possible to determine a speciation analysis using analytical chemistry methods alone. Thus utilizing chemical speciation models in conjunction with analytical methods are used in determination of chemical speciation.

Morel and Morgan 1972 has described in detail the multicomponent thermodynamic speciation modelling and has subsequently incorporated into publicly available software such as MINTEQ. The components are selected such that no component can be formed by a combination of other components and all species can be formed by the components. Thus mass balance for each component can be written and interrelationship among different components can be defined using mass action equation.

The components which are used in MINTEQ software are CH_3COO^- , Na^+ , Cl^- , NH_4^+ , K^+ , PO_4^{3-} , Mg^{2+} , SO_4^{2-} , Ca^{2+} , CO_3^{2-} , Fe^{2+} and H^+ .

The total concentration of each component in the system which is generally measured analytically equals the mass balances. Thus mass balance can be defined as

$$M_j = \sum_{i=1}^N A_{ij} \frac{x_i}{y_i}$$

Where

M_j is total mass of component j

A_{ij} is the stoichiometric coefficient giving the number of moles of component j in species i

x_i is the activity of the aqueous species i

y_i is the activity coefficient of species i

N is the number of components

Whereas the equilibrium constant (K) define the mass action equations which can be defined as

$$x_i = K_i \prod_{j=1}^N c_j^{A_{ij}}$$

where

K_i is the equilibrium constant for species i

The formation constant have been used from Joint Expert Speciation System (JESS) thermodynamic database (May, 2000; May and Murray, 2001). It should be noted here that speciation modelling is highly informative but it involves significant uncertainties (Nitzsche et al., 2000). Based on the aqueous phase speciation, the precipitation model has been developed to determine precipitate concentration. The solid species been considered are calcium phosphate and calcite.

The main model considerations are:

1. In aqueous phase the chemical equilibrium is quickly achieved in acid-base and ion pairing reaction. This assumption reduce simulation time (Rosen 2005) allowing determination of chemical equilibrium from set of algebraic equation. These equation depend on equilibrium constant for each reaction.
2. The solid formation reaction tend to equilibrium limited by rate of the process, but the model considers to be a fast reaction equilibrium thus overestimating considerably the precipitation.

Visual MINTEQ software was used which run on MINTEQA2 engine to model the aqueous phase.

3.8. Calculations

3.8.1. Alkalinity Mass Balance

In PSBR the alkalinity consumption of the algae bacteria consortium occurs due to algae photosynthesis and nitrification by autotrophs. During the algae photosynthesis, bicarbonate is been consumed by algae to produce oxygen which increases the pH in the reactor. Since pH controller is been used to control the pH at a set point pH of 7.3, 0.1 N HCL was been dosed whenever pH exceeds the limit. The addition of 0.1 HCl consumes the alkalinity in the mixed liquor of reactor. Mass balance of alkalinity was been done to calculate actual alkalinity consumption rate of algae bacteria consortium.

$$\begin{aligned} \text{Total Alkalinity(mol)} &= (V_e.C_a - V_x.C_{ab})/1000 \\ \text{or } (\mathbf{Alk_{act}}.(V_x + V_s) - V_x.C_{ab})/1000 \end{aligned}$$

Where:

- V_e = Unknown volume of 0.02N H₂SO₄ to be added for Alkali metric end point (ml)
- V_x = Volume of 0.1N HCL added to achieve set point pH of 7.3 (ml)
- C_a = Concentration of Standard Acid (0.02N H₂SO₄) [mol/L]
- C_{ab} =Concentration of acid used in pH controller (0.1N HCL) [mol/L]
- Alk_{act} =**Actual Alkalinity** when 0.1 HCl was not added(mol/L)
- V_s =Volume of Sample(ml)

$$\begin{aligned} \text{Total Alkalinity(mol)} &= \{ [HCO_3^-]_x + 2[CO_3^{2-}]_x + [A^-]_x + [OH^-]_x - [H^+]_x \} . (V_x + V_s)/1000 \\ \text{or } (\mathbf{Alk_{meas}}).(V_x + V_s)/1000 \end{aligned}$$

Where:

- V_s =Volume of Sample(ml)
- V_x = Volume of 0.1N HCL added to achieve set point pH of 7.3 (ml)

$[y]_x$ =Concentration of species y after addition of x ml of 0.1 N HCL (mol/L)
 Alk_{meas} =**Alkalinity measured(mol/L)**

$$\frac{(Alk_{act} \cdot (V_x + V_s) - V_x \cdot C_{ab})}{1000} = \frac{(Alk_{meas}) \cdot (V_x + V_s)}{1000}$$

$$Alk_{act} \cdot (V_x + V_s) = (Alk_{meas}) \cdot (V_x + V_s) + V_x \cdot C_{ab}$$

$$Alk_{act} = \frac{Alk_{meas} \cdot (V_x + V_s) + V_x \cdot C_{ab}}{V_x + V_s}$$

Since V_x is much smaller than V_s

$$\text{Therefore } Alk_{act} = \frac{Alk_{meas} \cdot V_s + V_x \cdot C_{ab}}{V_s}$$

$$Alk_{act} \text{ (mg CaCO}_3\text{/L)} = \frac{Alk_{meas} \cdot V_s + V_x \cdot C_{ab}}{V_s} \cdot 50,000$$

3.8.2. Ammonia Mass Balance

The initial concentration of ammonia in the PSBR is the average of ammonium concentration of effluent from the previous cycle and influent. The procedure to calculate the mass balance has been taken from (Karya et al., 2013).

Calculated/measured as follows	
Input	
Initial Ammonium-nitrogen (a)	$((NH_4^+ - N)_{feed \text{ reservoir}} + (NH_4^+ - N)_{effluent})/2$
Production and output	
Nitrate formed (b)	$[NO_3^- - N]_{\text{maximum observed during react phase}} - [NO_3^- - N]_{effluent}/2$
Ammonium uptake by nitrifiers(c)	Based on nitrogen content of biomass formed according to Eq 4
Ammonium uptake by algae (d)	$d = a - b - c$

3.8.3. Minimum Sludge Retention Time

The minimum SRT was calculated (Henze, M., et. al, 2008) as show below:

$$SRT_M = \frac{S}{\mu_{max} - b_A \cdot S}$$

where

s = Factor of safety

μ_{max} = Maximum specific growth rate of Nitrifiers at 32 °C

b_A = Endogenous Respiration Rate for Nitrifiers at 32 °C

Influent Temperature=	32 °C
Factor of Safety, s =	2
Endogenous Respiration Rate for Nitrifiers at 20 °C, b_{A20} =	0.04 /day
Endogenous Respiration Rate for Nitrifiers at 32 °C, b_{A32} =	0.056 /day

Assumptions: Reference (Henze et. al, 2008)

Maximum specific growth rate of Nitrifiers at 20 °C= 0.450 per day

Maximum specific growth rate of Nitrifiers at 32 °C= 1.810 per day

Minimum SRT required when operated in continuous reactor = **2.52** or **3.00** Day⁻¹

Since Reactor is Sequencing Batch Reactor (SBR) with 12hr cycle per day with only 6hr of nitrification occurring during the react stage.

The minimum SRT was therefore multiplied by factor 4 : (24/6)=4

Hence, Minimum SRT required for PSBR= 12 Days⁻¹

CHAPTER

4. Result and Discussion

4.1. Reactor 1 and 2: Biomass growth and environmental conditions

Two Photo Sequencing batch reactor [PSBR] were setup, the algae and sludge used to form algae bacteria consortia is shown in Figure 13 and its composition is shown in Table 8.

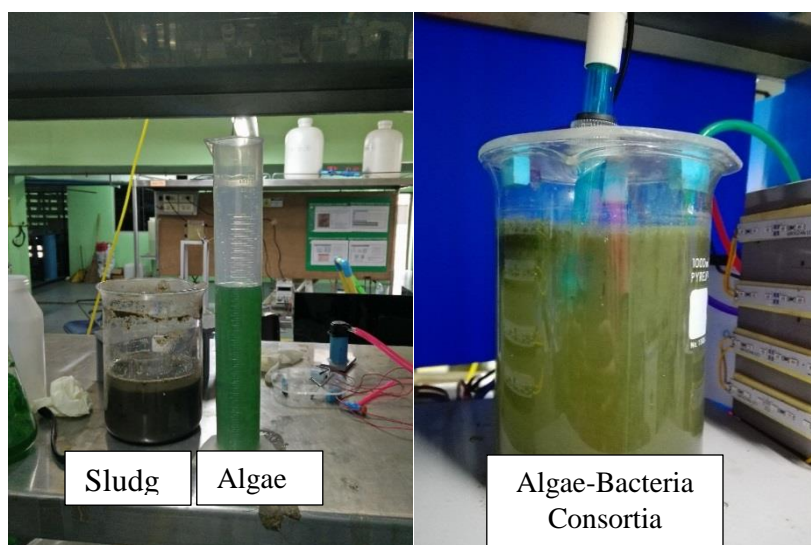


Figure 13 Algae Bacteria-Initial Composition

Table 8 Composition of Algae Bacteria

Particular	Volume	TSS	VSS		ISS	
	ml	mg/l	mg/l	%	mg/l	%
Algae	150	4312	644.4	15%	3667.6	85%
Sludge	350	3540	2282.5	64%	1257.5	36%
Actual Algae-Bacteria Consortia	1000	1997.5	570	29%	1428	71%

Initially both the reactors were fed with synthetic wastewater and operated for 12hr cycle per day with 11hr react time. In both the reactors pH controller was used at set point pH of 7.3 during Phase 1 which led to the formation of a well-settling flocs. The formation of flocs can be seen in Figure 14. During the study period no pure bacterial biomass aggregates were observed possibly because bacteria got attached to algae biomass or because small aggregates were washed out during decanting steps in the startup phase of operation. The majority of the biomass settled within 15 minutes, leaving relatively clear supernatant and low TSS. Thus algae-bacterial biomass indicated good settling ability.

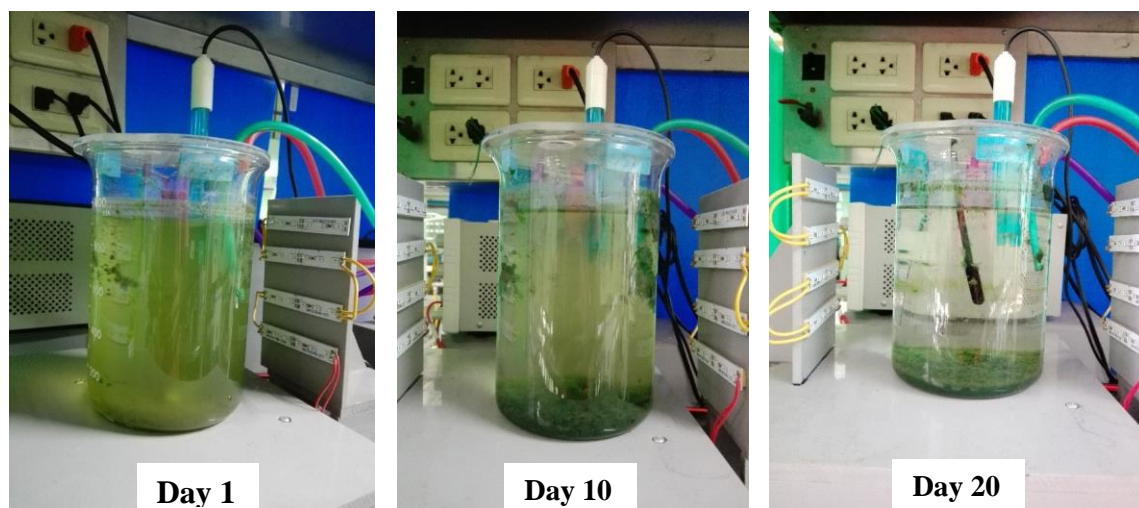


Figure 14 Algae bacteria flocs formation during the study Phase 1[30],Phase 2

The different operating conditions in phase 2 for the two PSBR as mentioned in Table 5 were maintained in the experimental study to evaluate the negative effect on the nitrification capacity of the algae bacteria consortia. The ammonium removal rate and alkalinity consumption rate in both the reactor was calculated in every phase by taking intermittent samples at defined intervals.

An SRT of 20 days was maintained in Phase 2 for both the reactors having 1 L capacity by removing 50ml of Mixed Liquor Suspended Solids (MLSS) at the end of the react stage in every cycle. Whereas no MLSS was removed at the end of the react stage during Phase 1 so as to prevent washout of nitrifiers from PSBRs. The average temperature during the react stage was 32° C .The TSS and VSS average concentration of mixed liquor inside the Reactor 1 is shown in Figure 15. Considering the entire operating time (Phase 1 and Phase 2) ,the TSS concentration of $1986 \pm 201 \text{ mg/L}$ and VSS concentration of $514 \pm 247 \text{ mg/l}$ were reported. The average VSS/TSS ratio in Reactor 1 was 26%.

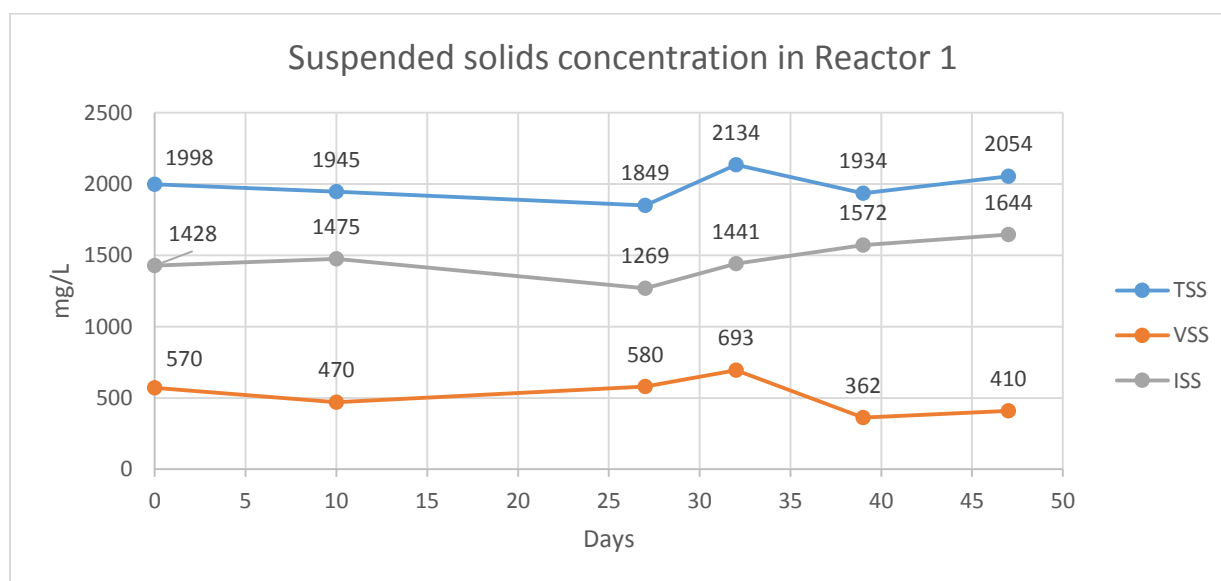


Figure 15 Suspended solids in Reactor 1 during Phase 1(30days), Phase 2a(6 days) and Phase 2b(10 Days)

Reactor 2 stopped nitrification on 13th day after the startup due to sludge accumulation in the pH sensor thus pH sensor reported higher value leading to increase in acid addition to control pH. This resulted in pH below 3 in Reactor 2 leading to the nonfunctioning of nitrifying biomass. Therefore Reactor 2 was started again with the same consortia of algae and bacteria as used previously in Reactor 1. The results of suspended solids in form of TSS, VSS and ISS in Reactor 2 is shown in Figure 16 it should be noted here that the reactor lags by 14 days to Reactor 1 because of the unforeseen circumstance as mentioned above. Reactor 2 has a TSS concentration of $1716 \pm 390 \text{ mg/L}$ and VSS concentration of $453 \pm 60 \text{ mg/L}$. The average VSS/TSS ratio in Reactor 2 was 26%.

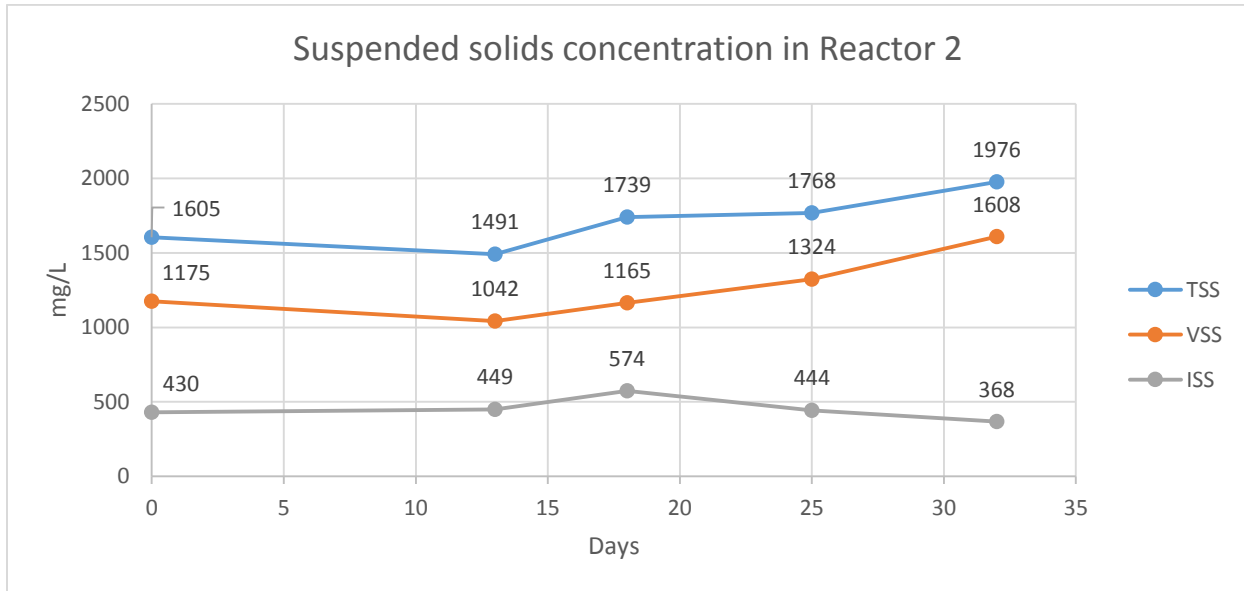


Figure 16 Suspended solids in Reactor 2 during Phase 1(16days), Phase 2a(6 days) and Phase 2b(10 Days)

4.2. Alkalinity Consumption rate

The alkalinity in Phase 1, 2a and 2b for Reactor 1 is shown in Figure 17 and Reactor 2 is shown in Figure 18. The alkalinity in the mixed liquor of both the reactors was measured in $\text{mg CaCO}_3/\text{L}$ during Phase 1 and Phase 2a was plotted against time for 3 days. In Phase 2b, the alkalinity measured for 5 days was plotted. The alkalinity is only measured during the first 6hr react period when there was considerable alkalinity. During the react time 6hr to 11hr, the alkalinity normally lies in the range of $50\text{--}150 \text{ mg CaCO}_3/\text{L}$. Since 0.1 N HCl was added by the pH controller to the PSBR which consumes the alkalinity, the actual consumption of alkalinity by algae bacteria consortiums is calculated by alkalinity mass balance. The actual alkalinity been consumed by algae-bacteria consortiums in different phases [1, 2a, 2b] after alkalinity mass balance for Reactor 1 is shown in Figure 19 and Reactor 2 is shown in Figure 20. The alkalinity mass balance for Phase 1, 2a and 2b of Reactor 1 and 2 is attached in **Appendix 1**.

Table 9 Alkalinity consumption rate (mgCaCO₃/L/hr) in PSBR

	Phase 1		Phase 2a		Phase 2b	
	Reactor 1	Reactor 2	Reactor 1	Reactor 2	Reactor 1	Reactor 2
	<u>Alkalinity consumption rate of algae bacteria consortiums</u> <u>(mgCaCO₃/L/hr)</u>					
1	65.83	59.17	86.25	71.25	114.14	81.72
2	106.00	121.50	84.00	81.75	111.12	81.60
3	73.50	50.50	60.25	61.50	113.92	108.53
4					129.09	85.52
5					137.97	92.72
Avg.	81.78	77.06	76.83	71.50	113.06	90.62
Stdev	21.32	38.73	14.41	10.13	11.70	11.29
Std. Error	±40.21	±73.04	±27.16	±19.10	±17.94	±17.31

The alkalinity consumption rate of algae-bacteria for Phase 1, 2a, 2b in Reactor 1 and Reactor 2 is calculated by averaging the slope of the linear function derived from Figure 19 and Figure 20. Reactor 1 and Reactor 2 alkalinity consumption rate is shown in Table 9 during the study period. In Phase 1, very high standard deviation can be observed in alkalinity consumption rate indicating the algae bacteria consumption was unstable initially. Whereas in Phase 2a and 2b the deviation is low. The oxygen generated by algae photosynthesis is sufficient for heterotrophs to consume organic matter [COD: 230 mg O₂/L] and autotrophs to carry out nitrification. The dissolved oxygen in the reactor was found to be around 2-3mg DO/L throughout the study period. The autotrophs also require inorganic carbon source in the form of bicarbonates for nitrification to occur. When the TSS concentration is high(>2g/L) the alkalinity consumption rate of the algae bacteria consortia increases which lead to low availability of bicarbonates for the nitrification to occur during the latter part of the react stage(4-6hr).

For the phosphorus removal via precipitation of calcium phosphate higher bicarbonate concentration decreases the removal efficiency. Thus biologically removing bicarbonates via algae photosynthesis and nitrification increases the phosphorus removal efficiency when pH is high. The low buffering capacity of the reactor, makes it very susceptible to pH change occurring due to nitrification (decreases pH) and algae photosynthesis (increases pH) when the pH is not controlled.

During the Phase 2 of the study, Reactor 1 was allowed to increase the pH by switching off the pH controller after 7 hours of react time for 4 hours. During which reactor 1 was able to achieve pH of 8.5(light intensity kept at 33 $\mu\text{mol}/\text{m}^2/\text{sec}$) and pH 9 (light intensity kept at 100 $\mu\text{mol}/\text{m}^2/\text{sec}$).It was observed that after 7hr of react time the alkalinity in the reactor is low(100-150mg CaCO₃/L) resulting in low buffering capacity of the reactor. Thus for a low consumption of bicarbonate via algae photosynthesis led to significant increase in pH.

It was found that maintaining an alkalinity above 80mg CaCO₃/L after 7hr of react time leads to an increase in pH biologically after pH controller was switched off. Whereas, when the alkalinity was lower than 80mg CaCO₃/L after 7hr react time in Phase 2, no increase in pH was observed. This highlights the importance of alkalinity consumption rate which determine the duration to keep pH controller on, to maintain minimum alkalinity for the pH to increase biologically. The pH controller should be switched off based on the alkalinity consumption of the PSBR for pH to increase biologically and achieve suitable condition for the calcium phosphate precipitation to occur.

It should also be noted here that in Phase 2, the SRT of 20 days is maintained and the TSS concentration was also stable. However, there was an increase in the alkalinity consumption rate when the bicarbonate concentration in the influent was high. This can be observed with lower alkalinity consumption rate in both reactors (Reactor 1-76.83±27.16 mgCaCO₃/L/hr; Reactor 2: 71.50±19.10 mgCaCO₃/L/hr) during Phase 2a, whereas in Phase2b (Reactor 1-113.06±17.94 mgCaCO₃/L/hr; Reactor 2: 90.62±17.31 mgCaCO₃/L/hr) showed higher consumption rate when bicarbonate concentration was higher.

The alkalinity consumption rate is also important to ensure there is enough bicarbonates available for the nitrifying biomass to carry out nitrification in the reactor. PSBR having high TSS leads to high alkalinity consumption rate in reactor apart from high concentration of bicarbonates in mixed liquor affecting the alkalinity consumption rate.

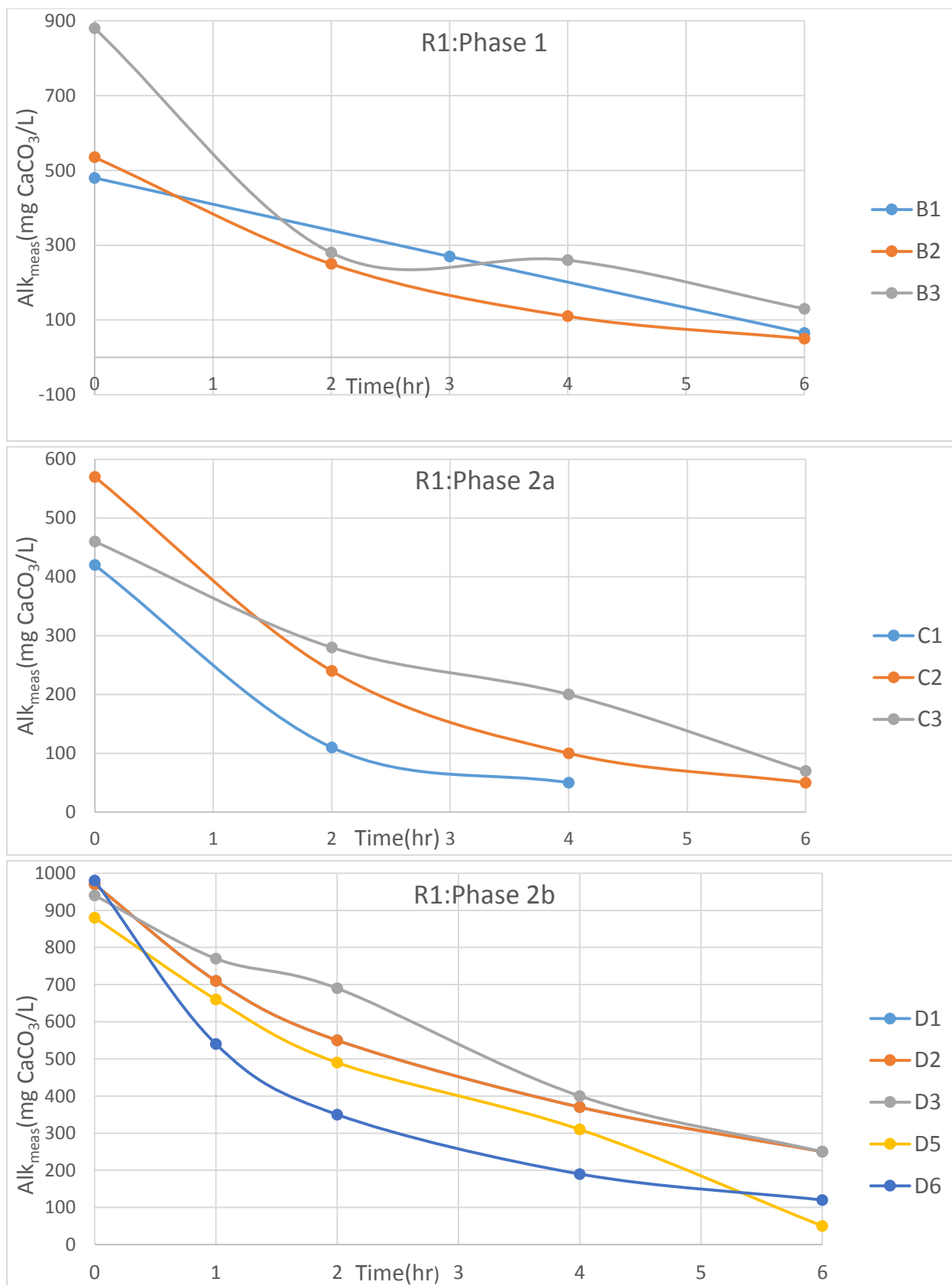


Figure 17 Measured Alkalinity in Reactor 1 during the study period

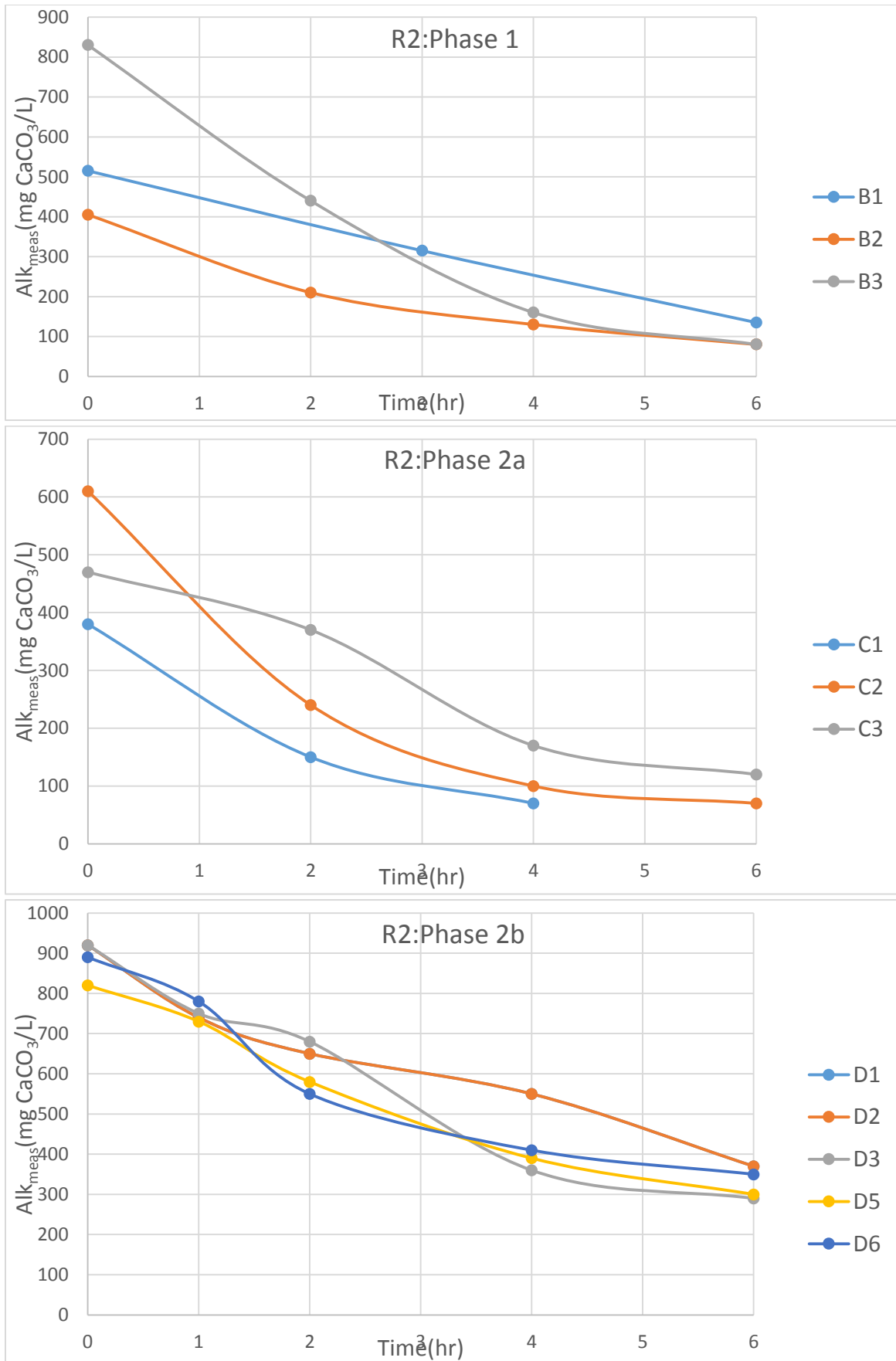


Figure 18 Measured Alkalinity in Reactor 2 during the study period

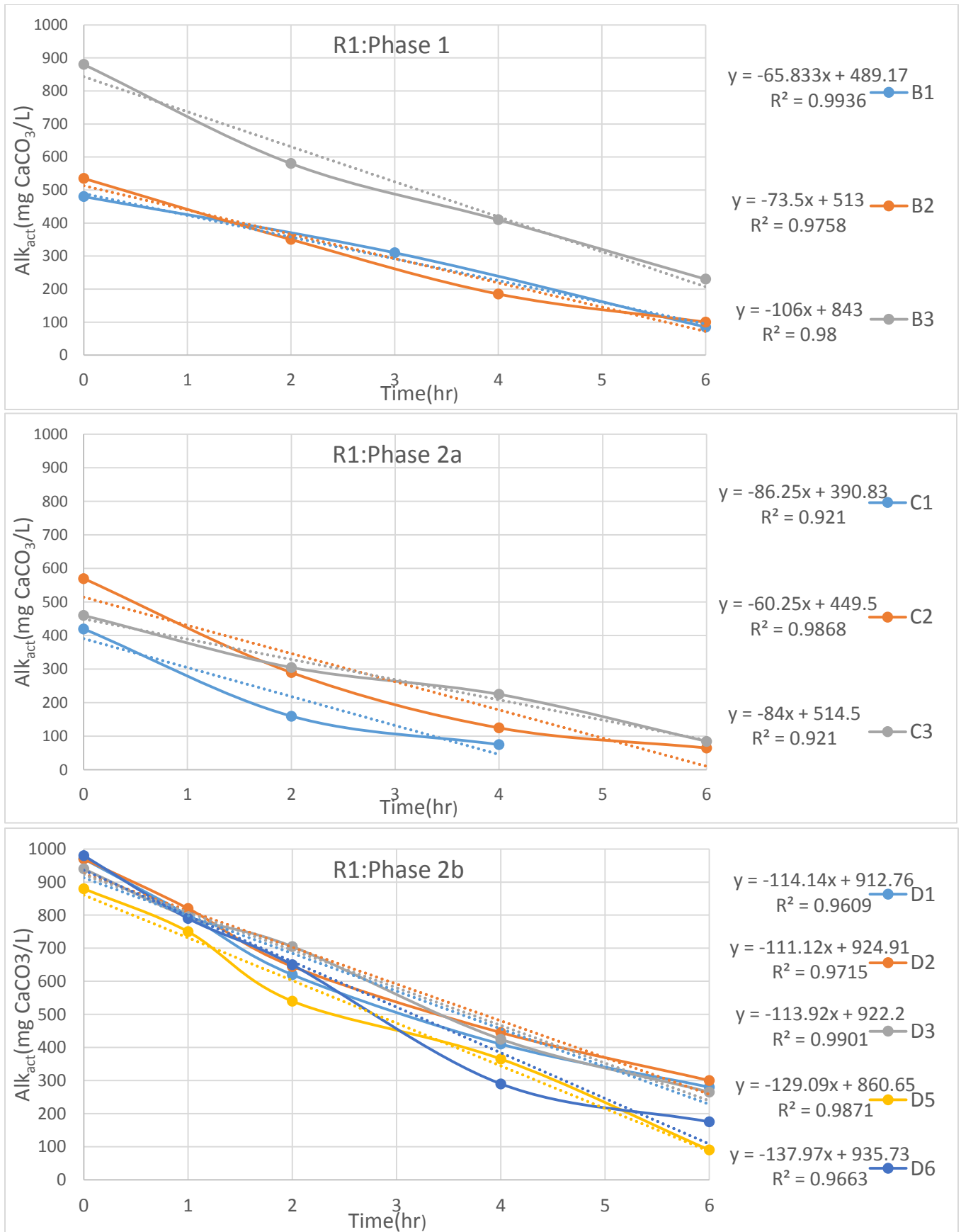


Figure 19 Alkalinity consumption in Reactor 1 during the study period

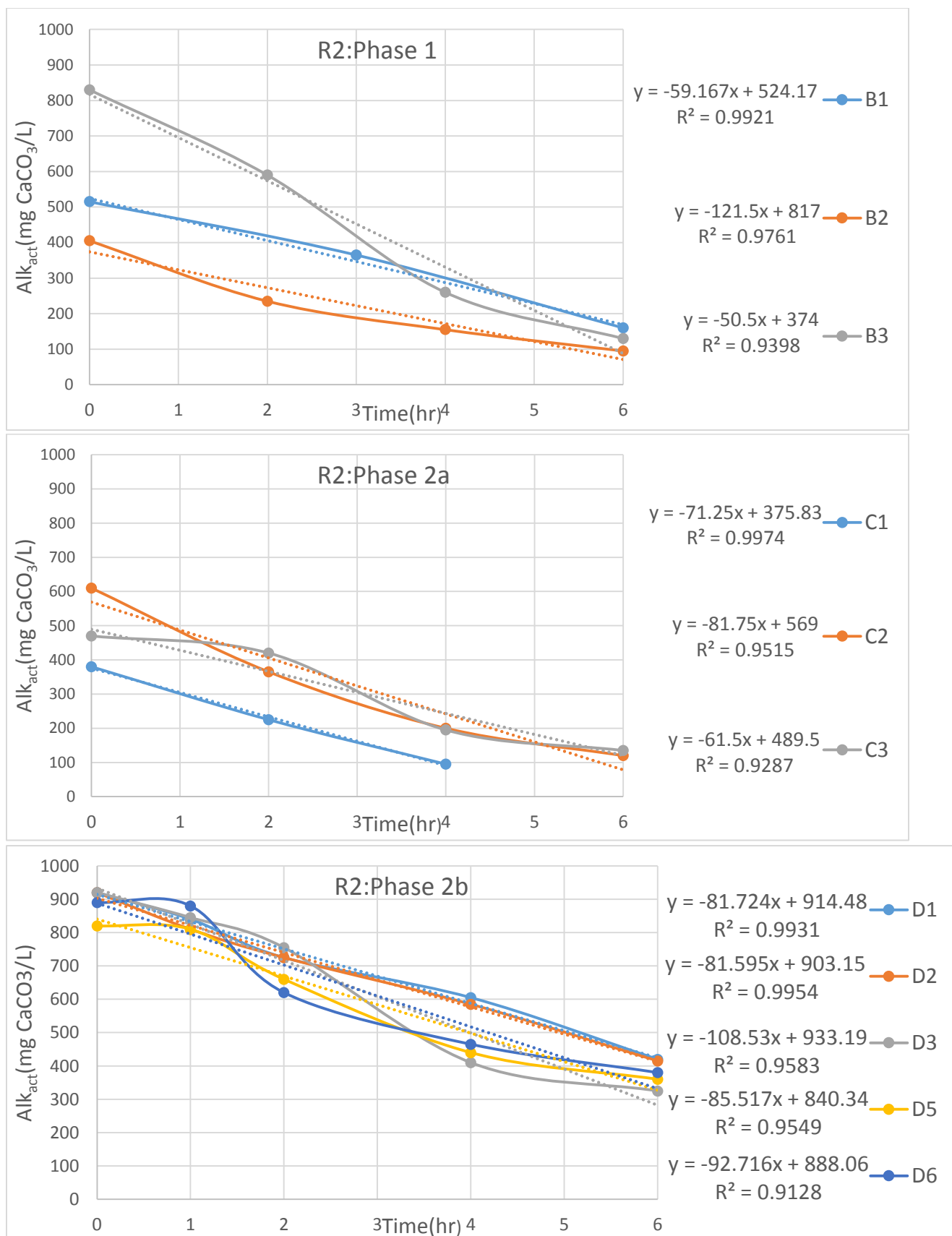


Figure 20 Alkalinity consumption in Reactor 2 during the study period

4.3. Ammonium removal rate in PSBR

The algae bacteria consortium in PSBR contain autotrophs which consume the bicarbonates to nitrify the ammonia to nitrates. The ammonia concentration of Reactor 1 in Phase 1,2a,2b is shown in Figure 21 and for Reactor 2 is shown in Figure 22. In both the figures the ammonia concentration is in mg $\text{NH}_4\text{-N/L}$ plotted against time in hours for 3 days in Phase 1,2a and for 5 days in Phase 2b. Ammonia is removed through nitrification by converting ammonia to nitrates and also uptake by algae and nitrifiers for biomass. The ammonium removal rate measured encompasses all the three processes.

The ammonium removal rate for Phase 1, 2a, 2b in Reactor 1 and Reactor 2 is calculated by averaging the slope of the linear slope derived from graph in Figure 21 and Figure 22 respectively as shown in Table 10. The pH in both the reactors was maintained at 7.3 using pH controller to facilitate nitrification. In Phase 1, the pH was controlled in both the reactors during the react time, whereas in Phase 2 the reactor 1 was kept at controlled pH, for first 7hr react time and for the next 4hr of react time, it was kept at uncontrolled pH.

Table 10 Ammonium Removal rate in PSBRs

	Phase 1		Phase 2a		Phase 2b	
	Reactor 1	Reactor 2	Reactor 1	Reactor 2	Reactor 1	Reactor 2
1	3.31	3.69	3.08	3.64	3.78	2.52
2	2.80	2.80	1.47	2.10	1.68	2.24
3	1.96	1.96	2.33	3.03	3.82	3.88
4					1.68	2.02
5					3.19	2.24
6					2.72	2.48
Avg.	2.69	2.82	2.29	2.92	2.53	2.25
St dev	0.56	0.71	0.66	0.63	0.63	0.19
Std. Error	±1.05	±1.33	±1.24	±1.19	±0.93	±0.28

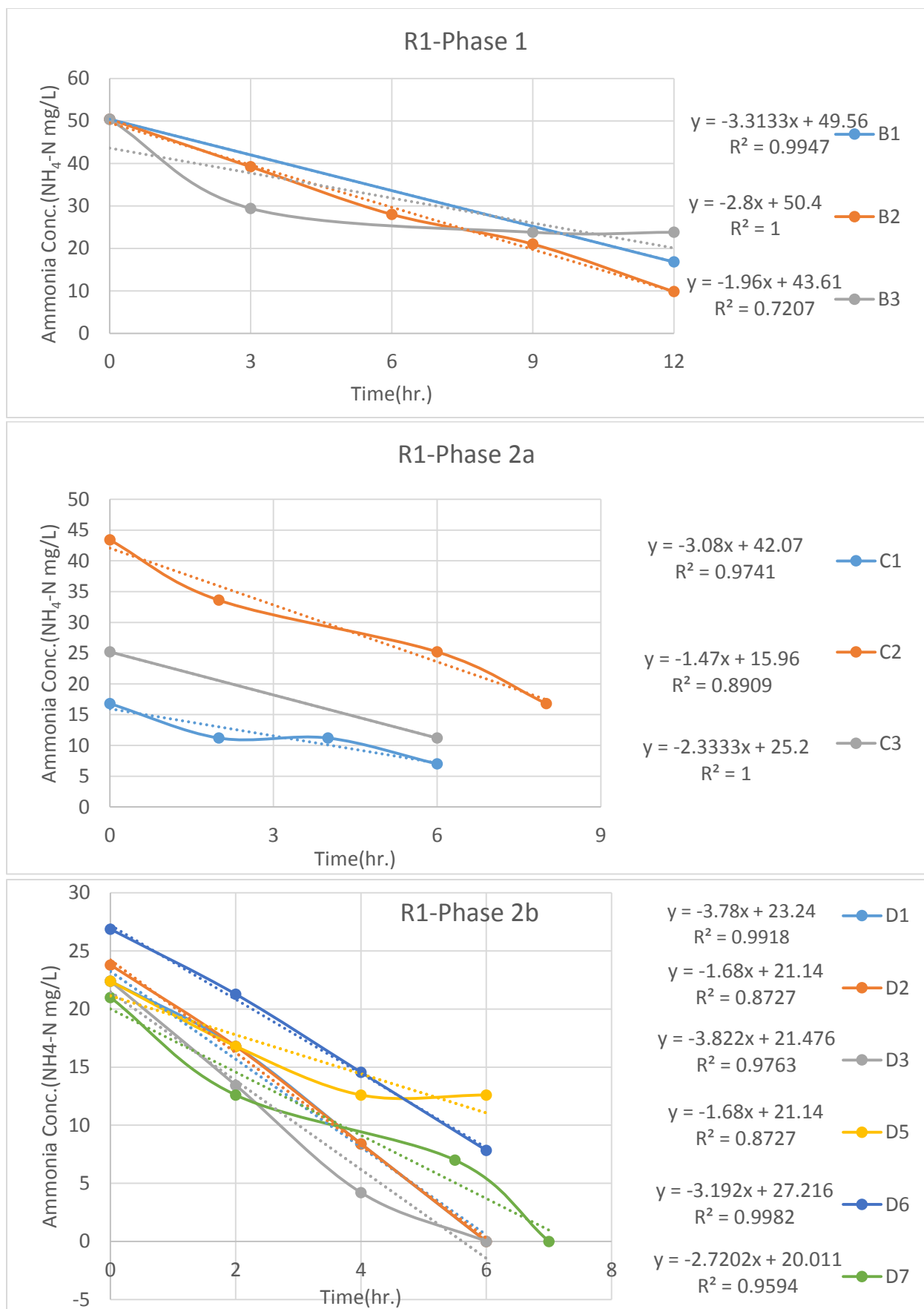


Figure 21 Ammonium Removal rate in Reactor 1 during the study period

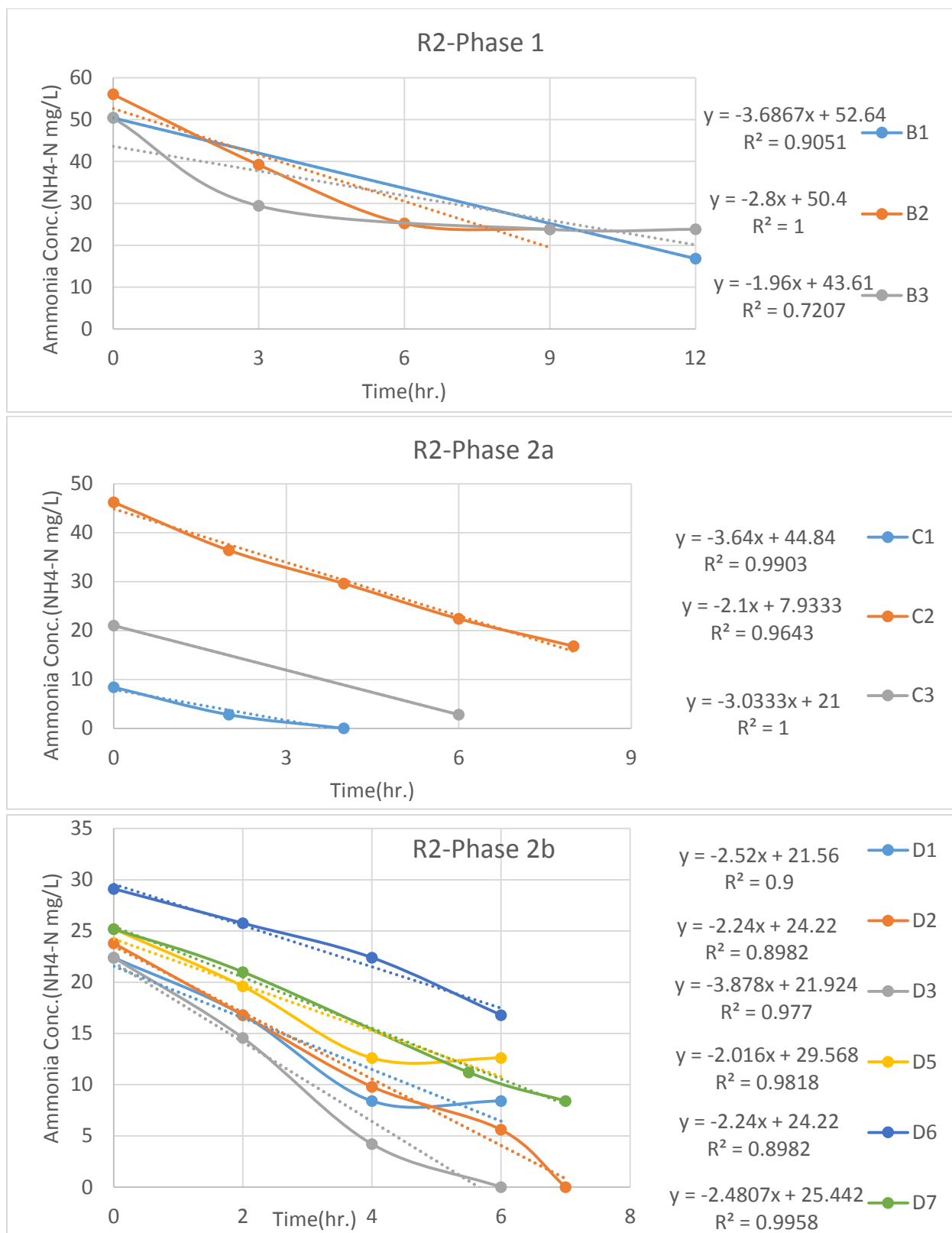


Figure 22 Ammonium removal rate in Reactor 2 during the study period

In Phase 2 it was noticed that when ammonia conc. is more than 20mg/L at the end of 5hr react period there was no increase in pH rather the pH dropped owing to the hydrogen ions produced due to nitrification. Typical graph of the pH for the above mentioned scenario is shown in Figure 23.

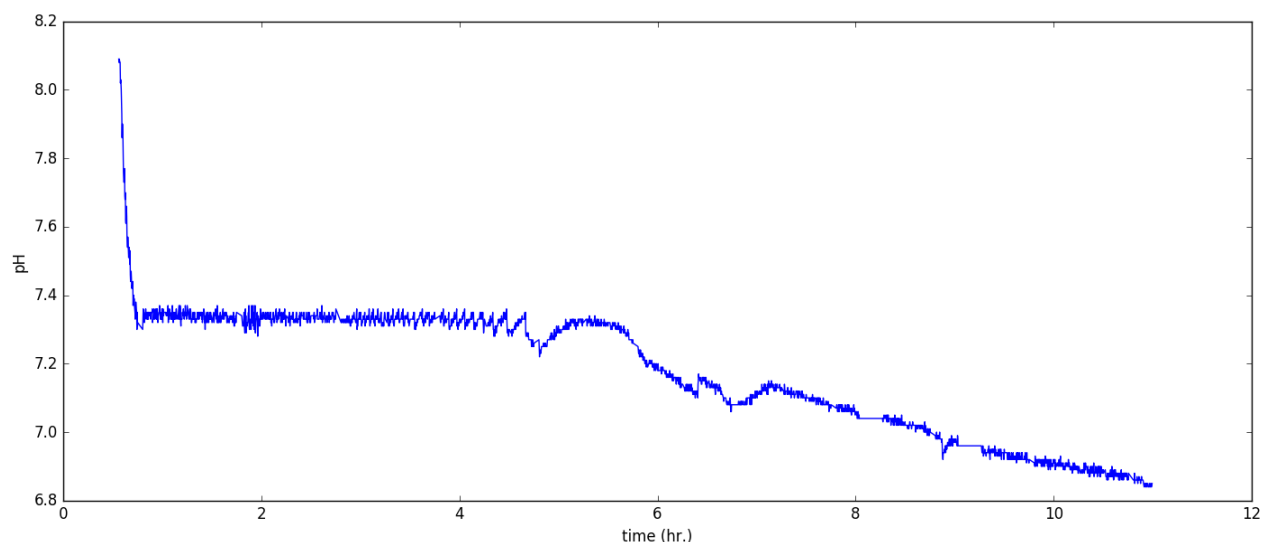


Figure 23 Typical pH decrease graph observed due to nitrification

Typical graph of increase in pH achieved biologically in Reactor 1 was show in Figure 27. The increase in pH was attributed to algae photosynthesis. The initial pH of the mixed liquor inside the reactor is 8.2-8.4 due to high alkalinity in the influent which is later adjusted to set point pH by pH controller. Since the ammonia gets typically depleted after 7hour react time when the pH controller is switched off, the algae utilizes Nitrates as nitrogen source.

Reactor 2 was kept at a controlled pH to compare the ammonia removal rate with Reactor 1 which achieved a high pH of 9. This was done to evaluate negative effect of increase in pH in the nitrification capacity of the PSBR. In phase 2b, the ammonium removal rate of Reactor 1 was 2.53 ± 0.93 ($p=0.1$) and Reactor 2 was 2.25 ± 0.28 ($p=0.1$), which indicates there is no negative effect in ammonium removal rate. However the ammonium removal rate is lower as compared to that reported by Karya et al., (2013) where an ammonium removal rate of 3.2 to 8.1 mg $\text{NH}_4\text{-N/hr}$ was observed. It should be noted here that no pure culture of nitrifiers was added to the system thus high concentration of nitrifiers could not be expected in the inoculum.

Since 21-23mg $\text{NH}_4^+\text{-N /L}$ is observed in the mixed liquor at the start of the reactor in phase 2b considering stoichiometry of nitrification reaction 1 mole of $\text{NH}_4^+\text{-N}$ produce 0.98 mole of $\text{NO}_3^-\text{-N}$. An average of 26.3 $\text{NO}_3^-\text{-N mg/L}$ was observed in Reactor 1 and 30.14 $\text{NO}_3^-\text{-N mg/L}$ in Reactor 2 during Phase 2b when the pH was increased to 9 and 8.5. The nitrate concentration of the effluent from Reactor 1 and 2 was plotted in Figure 24 for each day during Phase 2b. It can be clearly seen that there is no significant decrease in nitrate concentration thus supporting the above statement.

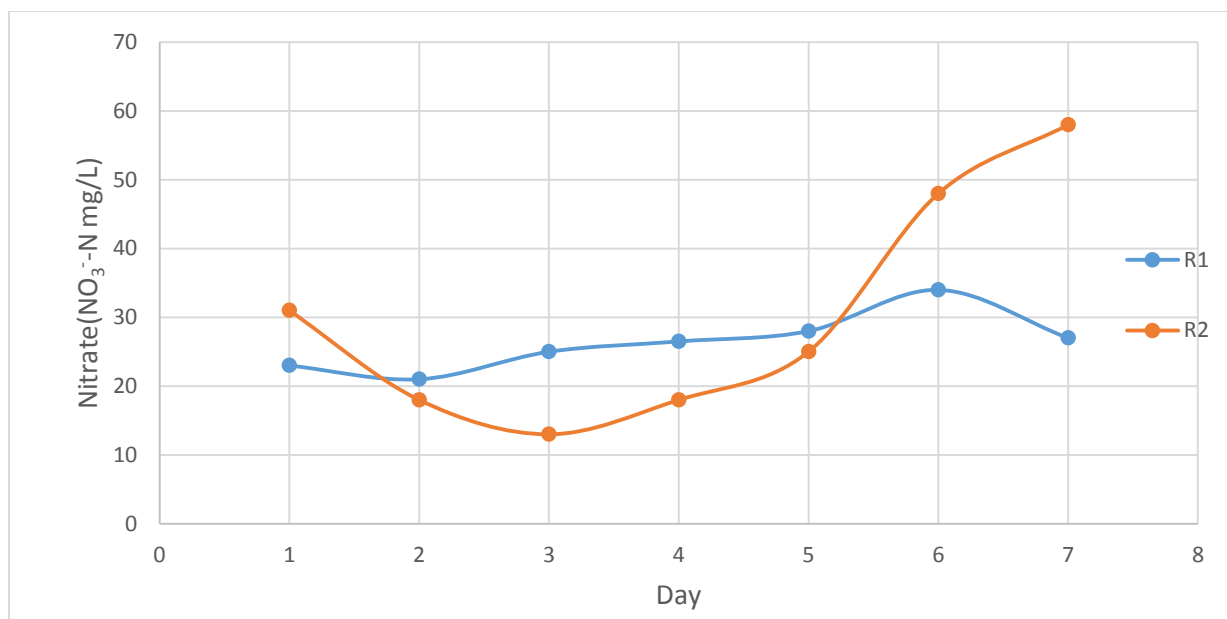


Figure 24 Nitrite Conc. in PSBRs during Phase 2b

4.4. Effect of solution condition on precipitation of calcium phosphate

Precipitation model has been developed using Visual MINTEQ to study the effect of solution condition on calcium phosphate precipitation. The precipitation calculation process conceptually first consist of the aqueous speciation and then determination of the precipitate concentration from speciation previously calculated. Each species is the product of the reaction involving only components. Thus the chemical representation is done using two characteristic variable which are species concentration (mmol L^{-1}) and component concentration (mmol L^{-1}) to adapt algebraic equation of the model to the equilibrium software (Visual MINTEQ). The concentration of each components in the mixed liquor of PSBR been observed at 0hr react time and 11 hr react time in Phase2a is shown in Table 12 and Table 13. For Phase 2b, the same is shown in Table 14 and Table 15. The possible solid phase been considered with their specified log activity and enthalpy (ΔH) is shown in Table 11. The aqueous phase reaction model is calculated as a chemical equilibrium problem kept at a temperature of 30 °C which was the average temperature inside the reactor during the study period. The typical temperature profile in the reactor is shown in Figure 25.

Table 11 Solid species: Specified log activity and Enthalpy

Species Name	Specified Fixed Log Activity	Enthalpy(ΔH)
Calcite	-8.48	-8
$\text{Ca}_3(\text{PO}_4)_2$ (am1)	-25.5	-94
$\text{Ca}_3(\text{PO}_4)_2$ (am2)	-28.25	-87
$\text{Ca}_3(\text{PO}_4)_2$ (beta)	-28.92	54
$\text{Ca}_4\text{H}(\text{PO}_4)_3 \cdot 3\text{H}_2\text{O}(\text{s})$	-47.95	-105
$\text{CaCO}_3 \cdot \text{H}_2\text{O}(\text{s})$	-7.144	-8
$\text{CaHPO}_4(\text{s})$	-19.275	31
$\text{CaHPO}_4 \cdot 2\text{H}_2\text{O}(\text{s})$	-18.995	23

The synthetic wastewater fed in Phase 2a is having following characteristic 50 mg N-NH₄⁺/L and 15 mg P-PO₄⁻³/L, 64.2 mg Ca⁺²/L, alkalinity 1618.9 mg CaCO₃/L. For Phase 2b, synthetic wastewater has following characteristic: 50 mg N-NH₄⁺/L, 15 mg P-PO₄⁻³/L, 1618.9 mg CaCO₃/L and 13 mg Ca⁺²/L.

In Phase 2a at the start of the react time the aqueous phase reaction model was performed based on the concentration of components derived from Table 12. The pH calculated from mass balance was 7.72 whereas the normal pH observed at 0hr React Phase 2a was 7.85-7.9. A charge difference of only 0.04% was found. The concentration and log activity of the aqueous inorganic species is shown in Table 16. The saturation index and mineral components is shown in Table 16. The calcium carbonate and calcium phosphate solid species were considered probable to precipitate in the model. The precipitate concentration calculated for calcite was 1.85m mol/L and Ca₃(PO₄)₂(beta) was 4.79x10⁻³ m mol/L. The distribution of components between the dissolved and precipitated phases is shown in Table 18. It should be noted here that only 0.23 mmol/L of Ca⁺² is dissolved in the reactor around 89% of calcium gets precipitated to calcite and calcium phosphate. Since calcite has a higher Log IAP than other calcium phosphate solid species therefore only 2% of phosphorus gets precipitated. This clearly indicates that carbonates are hindrance for phosphorus to be removed by precipitation as calcium phosphate.

The aqueous phase reaction model was performed for Phase 2a at react time 11hr based on the concentration of components derived from Table 13. A pH of 9 is observed at 11hr react time which is achieved via algae photosynthesis wherein bicarbonate ions have been consumed. The carbonate concentration shown in Table 13 is the alkalinity observed at react time 11 and the hydrogen ion concentration have been lowered to achieve pH based on the mass balance done by chemical equilibrium software. Since only 10% of calcium is dissolved in the mixed liquor of PSBR at 11hr therefore only 28.7% of phosphate gets precipitated as Ca₃(PO₄)₂(beta) having concentration of 6.76E-02 m mol/L, and no calcite precipitation was found.

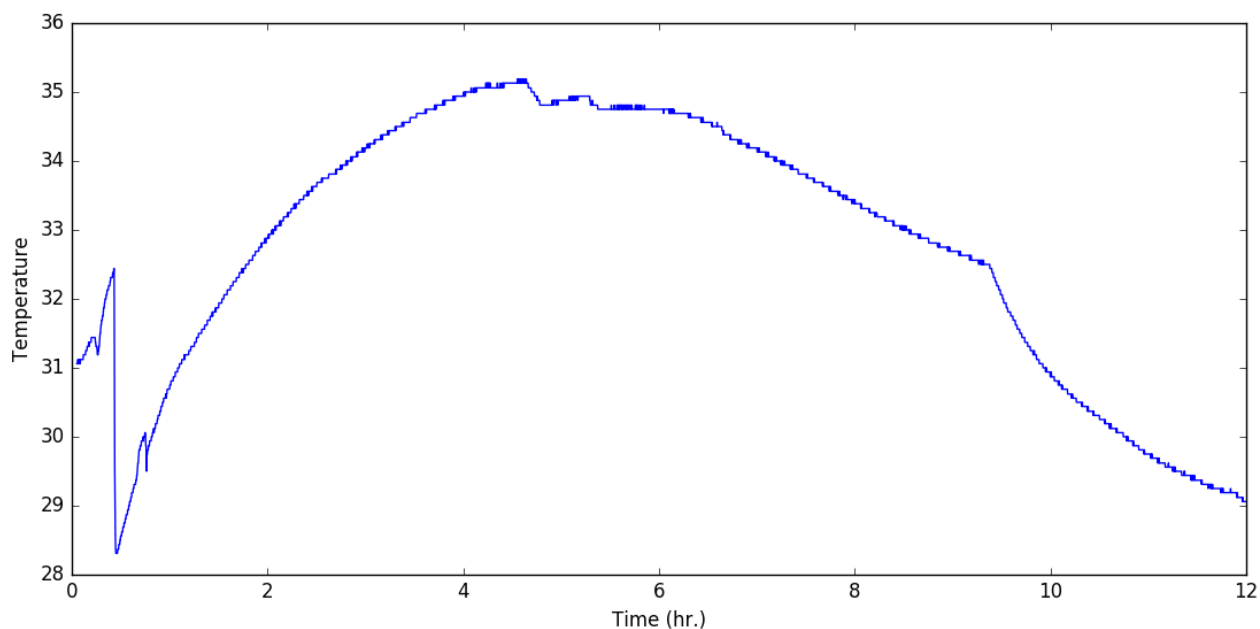


Figure 25 Typical Temperature profile during the study period

Table 12 Phase 2a: Stoichiometric matrix components and species at 0hr React Time

Species		mMol/L	CH ₃ COO ⁻	Na ⁺	Cl ⁻	NH ₄	K	PO ₄	Mg	SO ₄	Ca ⁺²	CO ₃	Fe ⁺²	H ⁺
Sodium Acetate	CH ₃ COONa	1.7968	1	1										
Citric Acid	C ₆ H ₈ O ₇ .H ₂ O													
Ammonium Chloride	NH ₄ Cl	1.8			1	1								
Di potassium phosphate	K ₂ HPO ₄	0.482					2	1						1
Magnesium Suplate	MgSO ₄ .7H ₂ O	0.6							1	1				
Calcium Chloride	CaCl ₂ .2H ₂ O	2.10			2						1			
Sodium Bicarbonate	NaHCO ₃	14.5		1								1		1
Ferrous Suplate	FeSO ₄ .7H ₂ O	0.02								1			1	
Sodium Carbonate	Na ₂ CO ₃	1.500		2								1		
<u>Total Conc.(mMol/L) of components</u>			<u>1.80</u>	<u>19.30</u>	<u>6.00</u>	<u>1.80</u>	<u>0.96</u>	<u>0.48</u>	<u>0.62</u>	<u>0.65</u>	<u>2.10</u>	<u>16.00</u>	<u>0.02</u>	<u>14.98</u>

Table 13 Phase 2a: Stoichiometric matrix components and species at 11hr React Time

Species		mMol/L	CH ₃ COO ⁻	Na ⁺	Cl ⁻	NH ₄	K	PO ₄	Mg	SO ₄	Ca ⁺²	CO ₃	Fe ⁺²	H ⁺
Sodium Acetate	CH ₃ COONa	0.0	1	1										
Ammonium Chloride	NH ₄ Cl	0.2			1	1								
Di potassium phosphate	K ₂ HPO ₄	0.482					2	1						1
Magnesium Suplate	MgSO ₄ .7H ₂ O	0.6							1	1				
Calcium Chloride	CaCl ₂ .2H ₂ O	2.10			2						1			
Sodium Bicarbonate	NaHCO ₃	1.4		1								1		1
Ferrous Suplate	FeSO ₄ .7H ₂ O	0.02								1			1	
Sodium Carbonate	Na ₂ CO ₃	0.0		2								1		
<u>Total Conc.(mMol/L) of components</u>			<u>0.00</u>	<u>1.40</u>	<u>4.40</u>	<u>0.20</u>	<u>0.96</u>	<u>0.48</u>	<u>0.62</u>	<u>0.65</u>	<u>0.23(2.1)</u>	<u>1.40</u>	<u>0.02</u>	<u>1.5(1.88)</u>

Table 14 Phase 2b: Stoichiometric matrix components and species at 0hr React Time

Components		mMol/L	CH ₃ COO ⁻	Na ⁺	Cl ⁻	NH ₄	K	PO ₄	Mg	SO ₄	Ca ⁺²	CO ₃	Fe ⁺²	H ⁺
Sodium Acetate	CH ₃ COONa	1.80	1	1										
Ammonium Chloride	NH ₄ Cl	1.8			1	1								
Di potassium phosphate	K ₂ HPO ₄	0.5					2	1						1
Magnesium Suplate	MgSO ₄ .7H ₂ O	0.6							1	1				
Calcium Chloride	CaCl ₂ .2H ₂ O	0.32			2						1			
Sodium Bicarbonate	NaHCO ₃	16.0		1								1		1
Ferrous Suplate	FeSO ₄ .7H ₂ O	0.02								1			1	
Sodium Carbonate	Na ₂ CO ₃	0.2		2								1		
<u>Total Conc.(mMol/L) of components</u>			<u>1.80</u>	<u>18.20</u>	<u>2.44</u>	<u>1.80</u>	<u>0.96</u>	<u>0.48</u>	<u>0.62</u>	<u>0.65</u>	<u>0.32</u>	<u>16.20</u>	<u>0.02</u>	<u>16.48</u>

Table 15 Phase 2b: Stoichiometric matrix components and species at 11hr React Time

Species		mMol/L	CH ₃ COO ⁻	Na ⁺	Cl ⁻	NH ₄	K	PO ₄	Mg	SO ₄	Ca ⁺²	CO ₃	Fe ⁺²	H ⁺
Sodium Acetate	CH ₃ COONa	0.00	1	1										
Ammonium Chloride	NH ₄ Cl	0.2			1	1								
Di potassium phosphate	K ₂ HPO ₄	0.482					2	1						1
Magnesium Suplate	MgSO ₄ .7H ₂ O	0.6							1	1				
Calcium Chloride	CaCl ₂ .2H ₂ O	2.10			2						1			
Sodium Bicarbonate	NaHCO ₃	0.0		1								1		1
Ferrous Suplate	FeSO ₄ .7H ₂ O	0.02								1			1	
Sodium Carbonate	Na ₂ CO ₃	1.400		2								1		
<u>Total Conc.(mMol/L) of components</u>			<u>0.00</u>	<u>2.80</u>	<u>4.43</u>	<u>0.23</u>	<u>0.96</u>	<u>0.48</u>	<u>0.62</u>	<u>0.65</u>	<u>2.10</u>	<u>1.40</u>	<u>0.02</u>	<u>0.15(0.48)</u>

Table 16 Saturation Index and Mineral Components of PSBR in Phase2a at React Time 0 hr

Mineral	log IAP	Sat. index	Stoichiometry and Mineral Components							
Ca ₃ (PO ₄) ₂ (am1)	-28.764	-2.992	3	Ca+2	2	PO4-3				
Ca ₃ (PO ₄) ₂ (am2)	-28.764	-0.263	3	Ca+2	2	PO4-3				
Ca ₃ (PO ₄) ₂ (beta)	-28.764	0	3	Ca+2	2	PO4-3				
Ca ₄ H(PO ₄) ₃ :3H ₂ O(s)	-48.864	-0.61	4	Ca+2	1	H+1	3	PO4-3	3	H ₂ O
CaCO ₃ xH ₂ O(s)	-8.51	-1.323	1	Ca+2	1	CO ₃ -2	1	H ₂ O		
CaHPO ₄ (s)	-20.099	-0.913	1	Ca+2	1	H+1	1	PO4-3		
CaHPO ₄ :2H ₂ O(s)	-20.099	-1.171	1	Ca+2	1	H+1	1	PO4-3	2	H ₂ O
Calcite	-8.51	0	1	Ca+2	1	CO ₃ -2				

Table 17 Saturation Index and Mineral Components of PSBR in Phase2a at React Time 11 hr

Mineral	log IAP	Sat. index	Stoichiometry and Mineral Components							
Ca ₃ (PO ₄) ₂ (am1)	-28.764	-2.992	3	Ca+2	2	PO4-3				
Ca ₃ (PO ₄) ₂ (am2)	-28.764	-0.263	3	Ca+2	2	PO4-3				
Ca ₃ (PO ₄) ₂ (beta)	-28.764	0	3	Ca+2	2	PO4-3				
Ca ₄ H(PO ₄) ₃ :3H ₂ O(s)	-49.773	-1.52	4	Ca+2	1	H+1	3	PO4-3	3	H ₂ O
CaCO ₃ xH ₂ O(s)	-9.072	-1.885	1	Ca+2	1	CO ₃ -2	1	H ₂ O		
CaHPO ₄ (s)	-21.009	-1.823	1	Ca+2	1	H+1	1	PO4-3		
CaHPO ₄ :2H ₂ O(s)	-21.009	-2.08	1	Ca+2	1	H+1	1	PO4-3	2	H ₂ O
Calcite	-9.072	-0.562	1	Ca+2	1	CO ₃ -2				

Table 18 Distribution of Components between dissolved and precipitated phases of PSBR in Phase2 at React Time 0

Component	Total dissolved	% dissolved	Total precipitated	% precipitated
Acetate-1	0.00180	100.0	0.000	0.00
Ca+2	0.00023	10.9	0.002	89.09
Cl-1	0.00600	100.0	0.000	0.00
CO ₃ -2	0.01414	88.4	0.002	11.60
Fe+2	0.00002	100.0	0.000	0.00
H+1	0.01500	100.0	0.000	0.00
K+1	0.00096	100.0	0.000	0.00
Mg+2	0.00062	100.0	0.000	0.00
Na+1	0.01930	100.0	0.000	0.00
NH ₄ +1	0.00180	100.0	0.000	0.00
PO ₄ -3	0.00047	98.0	0.000	2.00
SO ₄ -2	0.00065	100.0	0.000	0.00

Table 19 Distribution of Components between dissolved and precipitated phases of PSBR in Phase2 at React Time 11

Component	Total dissolved(mol/L)	% dissolved	Total precipitated	% precipitated
Acetate-1	0.00000	100.0	0.000	0.00
Ca+2	0.00003	11.4	0.000	88.62
Cl-1	0.00440	100.0	0.000	0.00
CO3-2	0.00139	100.0	0.000	0.00
Fe+2	0.00002	100.0	0.000	0.00
H+1	0.00145	100.0	0.000	0.00
K+1	0.00096	100.0	0.000	0.00
Mg+2	0.00062	100.0	0.000	0.00
Na+1	0.00550	100.0	0.000	0.00
NH4+1	0.00023	100.0	0.000	0.00
PO4-3	0.00033	71.2	0.000	28.77
SO4-2	0.00065	100.0	0.000	0.00

The concentration of components derived from Table 14 was used to model the aqueous phase in Phase 2b at react time 0 hr. The pH calculated from mass balance is 8.07 whereas the normal pH observed at the start of Phase 2b was 8.3-8.4. All the species concentration here are similar from Phase 2a except CaCl₂ which is 0.32mmol/L. The aqueous phase reaction model was performed to give precipitate of only calcite as solid species having a concentration of 0.222m mol/L. The saturation index and mineral components is shown in Table 20. Since there is not enough concentration of calcium ions saturation index of calcium phosphate solid species is less than zero. The distribution of components between the dissolved and precipitated phases is shown in Table 22.

The aqueous phase reaction model was again performed in Phase 2b at react time 11 hr. A pH of 9 is observed at 11hr react time which is achieved by similar process as mentioned above in Phase 2a. The carbonate concentration shown in Table 15 is the alkalinity observed at react time 11 and the hydrogen ion concentration have been lowered to achieve pH based on the mass balance done by chemical equilibrium software. Calcium chloride had been dosed to the mixed liquor of PSBR to achieve a concentration of 2.1mmol/L. It was seen that 98% of phosphorus precipitated as shown in Table 23. Thus increasing the calcium concentration when the carbonate concentration is high increase the removal efficiency of phosphate.

Table 20 Saturation Index and Mineral Components of PSBR in Phase2b at React Time 0 hr

Mineral	log IAP	Sat. index	Stoichiometry and Mineral Components							
Ca ₃ (PO ₄) ₂ (am1)	-29.181	-3.41	3	Ca+2	2	PO4-3				
Ca ₃ (PO ₄) ₂ (am2)	-29.181	-0.68	3	Ca+2	2	PO4-3				
Ca ₃ (PO ₄) ₂ (beta)	-29.181	-0.417	3	Ca+2	2	PO4-3				
Ca ₄ H(PO ₄) ₃ :3H ₂ O(s)	-49.632	-1.379	4	Ca+2	1	H+1	3	PO4-3	3	H ₂ O
CaCO ₃ xH ₂ O(s)	-8.51	-1.323	1	Ca+2	1	CO ₃ -2	1	H ₂ O		
CaHPO ₄ (s)	-20.45	-1.265	1	Ca+2	1	H+1	1	PO4-3		
CaHPO ₄ :2H ₂ O(s)	-20.451	-1.522	1	Ca+2	1	H+1	1	PO4-3	2	H ₂ O
Calcite	-8.51	0	1	Ca+2	1	CO ₃ -2				

Table 21 Saturation Index and Mineral Components of PSBR in Phase2b at React Time 11 hr

Mineral	log IAP	Sat. index	Stoichiometry and Mineral Components							
Ca ₃ (PO ₄) ₂ (am1)	-28.764	-2.992	3	Ca+2	2	PO4-3				
Ca ₃ (PO ₄) ₂ (am2)	-28.764	-0.263	3	Ca+2	2	PO4-3				
Ca ₃ (PO ₄) ₂ (beta)	-28.764	0	3	Ca+2	2	PO4-3				
Ca ₄ H(PO ₄) ₃ :3H ₂ O(s)	-50.364	-2.111	4	Ca+2	1	H+1	3	PO4-3	3	H ₂ O
CaCO ₃ xH ₂ O(s)	-8.51	-1.323	1	Ca+2	1	CO ₃ -2	1	H ₂ O		
CaHPO ₄ (s)	-21.6	-2.414	1	Ca+2	1	H+1	1	PO4-3		
CaHPO ₄ :2H ₂ O(s)	-21.6	-2.671	1	Ca+2	1	H+1	1	PO4-3	2	H ₂ O
Calcite	-8.51	0	1	Ca+2	1	CO ₃ -2				

Table 22 Distribution of Components between dissolved and precipitated phases of PSBR in Phase2b at React Time 0

Component	Total dissolved(mol/L)	% dissolved	Total precipitated	% precipitated
Acetate-1	0.00180	100.0	0.000	0.00
Ca+2	0.00009	29.5	0.000	70.47
Cl-1	0.00244	100.0	0.000	0.00
CO ₃ -2	0.01597	98.6	0.000	1.39
Fe+2	0.00002	100.0	0.000	0.00
H+1	0.01640	100.0	0.000	0.00
K+1	0.00096	100.0	0.000	0.00
Mg+2	0.00062	100.0	0.000	0.00
Na+1	0.01817	100.0	0.000	0.00
NH ₄ +1	0.00180	100.0	0.000	0.00
PO ₄ -3	0.00048	100.0	0.000	0.00
SO ₄ -2	0.00065	100.0	0.000	0.00

Table 23 Distribution of Components between dissolved and precipitated phases of PSBR in Phase2b at React Time 11

Component	Total dissolved(mol/L)	% dissolved	Total precipitated	% precipitated
Acetate-1	0.00000	100.0	0.000	0.00
Ca+2	0.00033	15.6	0.002	84.44
Cl-1	0.00420	100.0	0.000	0.00
CO3-2	0.00031	22.4	0.001	77.63
Fe+2	0.00002	100.0	0.000	0.00
H+1	0.00015	100.0	0.000	0.00
K+1	0.00096	100.0	0.000	0.00
Mg+2	0.00062	100.0	0.000	0.00
Na+1	0.00280	100.0	0.000	0.00
NH4+1	0.00023	100.0	0.000	0.00
PO4-3	0.00001	1.2	0.000	98.76
SO4-2	0.00065	100.0	0.000	0.00

4.5. Phosphorus removal

The phosphorus removal in the PSBR was achieved in Phase 2 wherein Reactor 1 was kept at uncontrolled pH for 4 hr. to achieve a pH increase up to 9.

In Phase 2a, initially high concentration of calcium was present but this could not result in phosphorus removal in both the reactor because of high carbonate concentration in the mixed liquor which led to calcite formation resulting in no significant phosphorus removal. This was validated by MINTEQ2 software simulation as shown in were calcite had higher saturation index than calcium phosphate there was also no significant phosphorus uptake by the algae-bacteria biomass observed as show in the Figure 26 below.

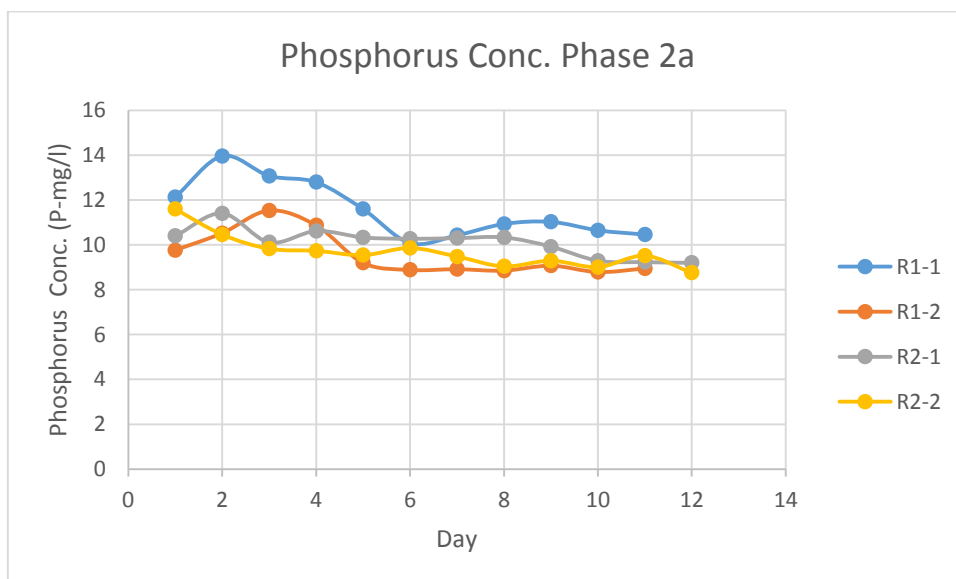


Figure 26 Phosphorus Concentration in PSBR during Phase 2a

In Phase 2b, the reactor was fed with low calcium concentration which resulted in no significant calcite and calcium phosphate precipitation at React time 0Hr as shown in Table 19. Reactor 1 was kept at uncontrolled pH for four hours during the latter part of react period when majority of the ammonia was removed. During this period when a light intensity of 35-30 $\mu\text{mol}/\text{m}^2/\text{sec}$ was provided pH of 8.5 was achieved. Whereas when light intensity was increased to 95-100 $\mu\text{mol}/\text{m}^2/\text{sec}$ a pH of 9 was achieved.. The pH increase achieved upto 9.1 pH at the end of react period when light intensity of 95-100 $\mu\text{mol}/\text{m}^2/\text{sec}$ was provided as shown in Figure 27 below.

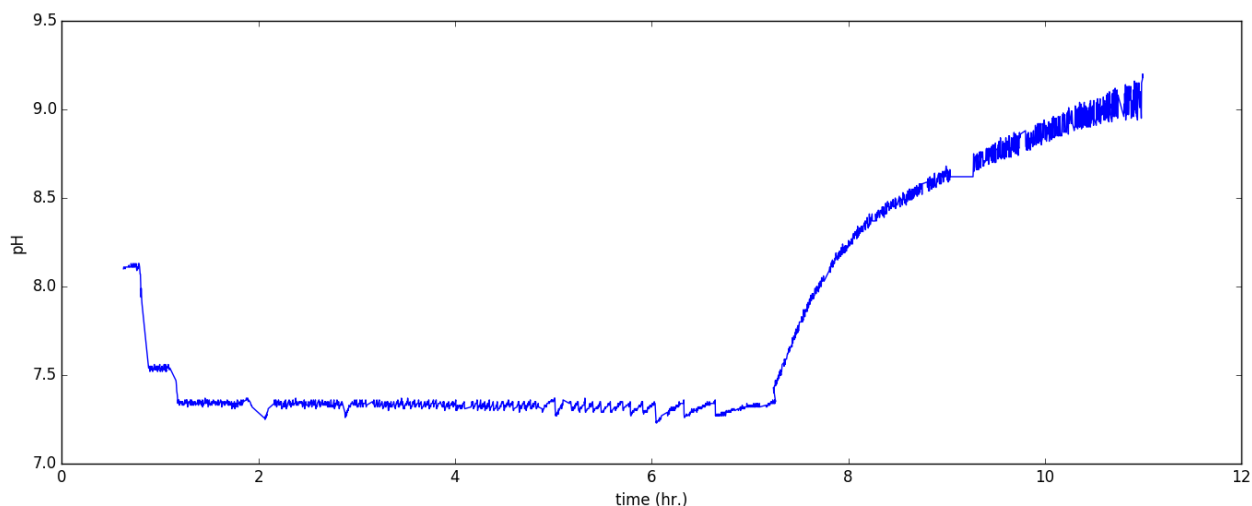


Figure 27 Typical pH increase achieved in Reactor 1 during Phase2b

Reactor 2 was kept at controlled pH throughout the 11hr react period with a light intensity of 35-30 $\mu\text{mol}/\text{m}^2/\text{sec}$, therefore pH 7.3 was observed .At the end of the react period 10ml of 0.2M calcium chloride was dosed to the mixed liquor in both the reactors to achieve a concentration of 2.12mM Ca^{+2} in the mixed liquor. The phosphorus concentration at the end of the settling period was analyzed. The phosphorus concentration at the start of react period, at 11hr react period after CaCl_2 had been dosed and at the end of the settling period for both the PSBR were analyzed. The phosphorus concentration at different time interval as mentioned above for Reactor 1 is shown in Figure 28 and Reactor 2 is shown in Figure 29.

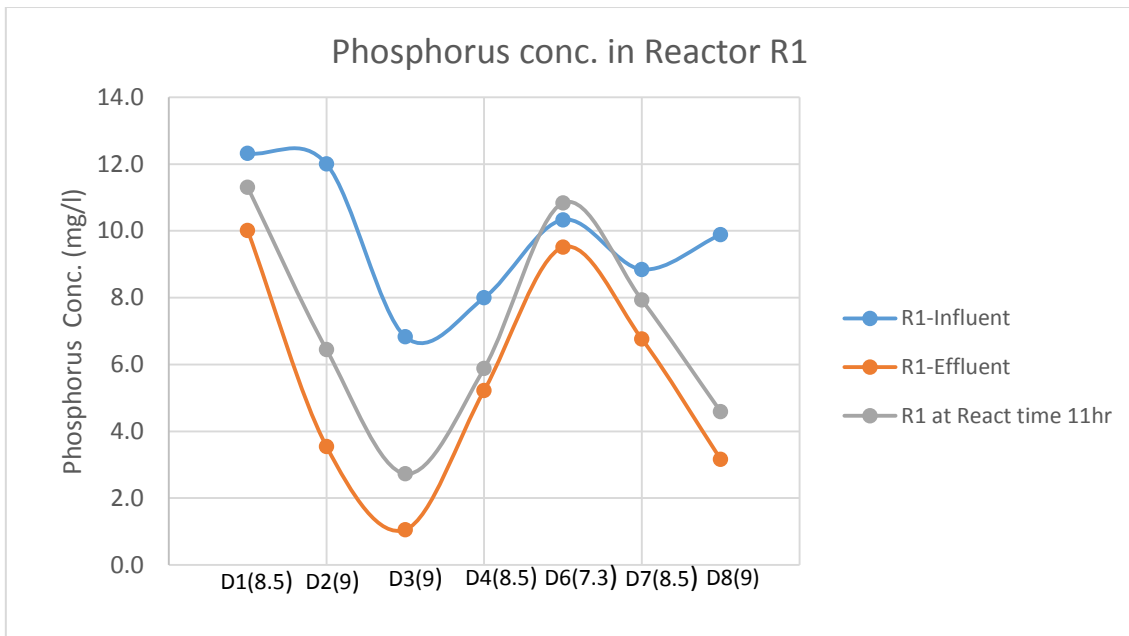


Figure 28 Phosphorus Conc. at different React Period in Reactor 1 during Phase 2b

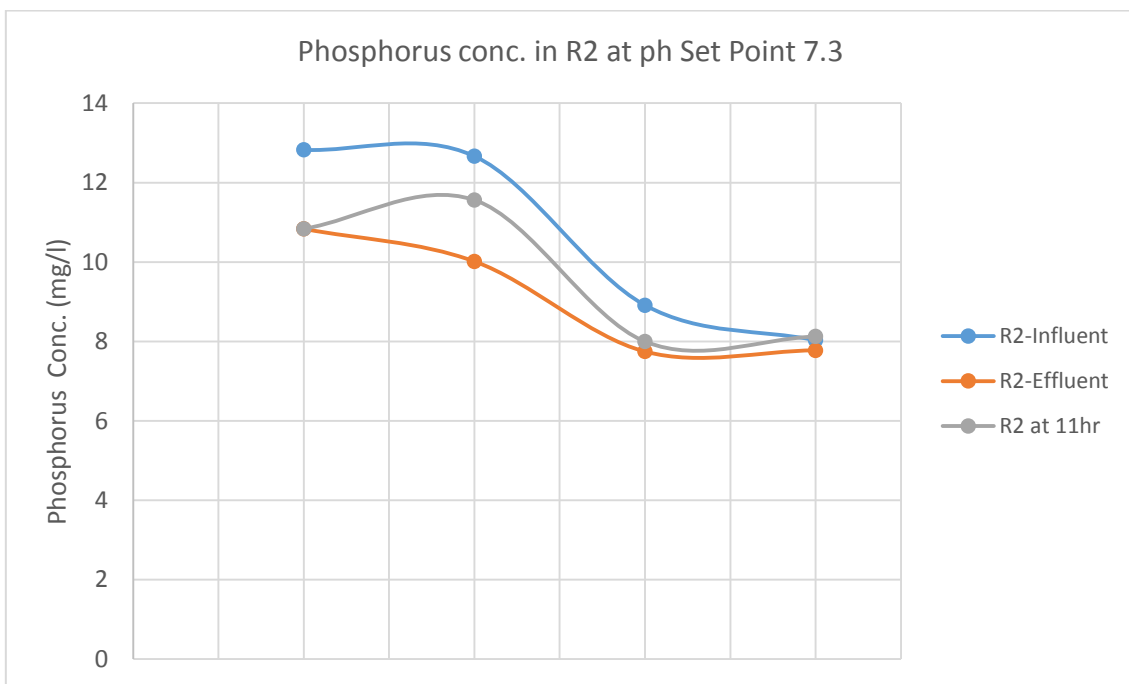


Figure 29 Phosphorus Conc. at different React Period in Reactor 2 during Phase 2b

The removal efficiency observed during Phase 2b with different pH achieved at the end of react period for Reactor 1 is shown in Table 24. The removal efficiency of Reactor 2 with pH set point 7.3 is shown in Table 25.

Table 24 Phosphorus removal efficiency observed in Reactor 1 during Phase 2b

Nomenclature	Time(hr)	P-PO ₄ ⁻³ (mg/l)	Removal Efficiency (Inff-Eff)/Inff	pH Achieved
D1	0'	12.3	19%	8.5
	11'	11.3		
	11'30"	10.0		
D2	0'	12.0	70%	9
	11'	6.5		
	11'30"	3.5		
D3	0'	6.8	85%	9
	11'	2.7		
	11'30"	1.1		
D4	0'	8.0	35%	8.5
	11'	5.9		
	11'30"	5.2		
D6	0'	10.3	8%	7.3
	11'	10.8		
	11'30"	9.5		
D7	0'	8.8	24%	8.5
	11'	7.9		
	11'30"	6.8		
D8	0'	9.9	68%	9
	11'	4.6		
	11'30"	3.2		

Table 25 Phosphorus Removal Efficiency achieved in Reactor 2 during Phase 2b

Nomenclature	Time(hr)	P-PO ₄ ⁻³ (mg/l)	Removal Efficiency (Inff-Eff)/Inff	pH Achieved
D1	0'	12.8	15%	7.3
	11'	10.8		
	11'30"	10.8		
D2	0'	12.7	21%	7.3
	11'	11.6		
	11'30"	10.0		
D3	0'	8.9	13%	7.3
	11'	8.0		
	11'30"	7.7		
D4	0'	8.0	3%	7.3
	11'	8.1		
	11'30"	7.8		

The overall removal efficiency observed in both reactor with p=0.05 at different pH achieved at the end of the react period is shown in the Table 26.

Table 26 Phosphorus Removal Efficiency in PSBR with different pH achieved at the end of React Period during Phase 2b

At pH	Removal Efficiency (Inff-Eff)/Inff
7.3 (Reactor 2)	13.1% \pm 3%
8.5 (Reactor 1)	25.6% \pm 7%
9 (Reactor 1)	74.3% \pm 19%

It can be clearly seen that higher removal efficiency of 74.31% \pm 19% was observed at pH 9. The aqueous phase reaction model predicted a removal of 98.76% \pm 19% at pH 9 with similar solution condition. The model overestimated considerably the precipitation since fast reaction does not occur in many heterogeneous equilibriums such as the precipitation. The reaction rate of the processes which are precipitation and dissolution should be taken into account. The kinetics of the process are mostly surface controlled so an increase in removal efficiency can be expected in the batch reactor where significant calcium phosphate precipitation occurs in the previous cycles. The reaction rate is insensitive to the fluid dynamics and observed relatively high activation energy point to surface controlled crystallization (Koutsoukos et al., 1979).

The phosphorus removal by phosphorus accumulating organism doesn't occur since it requires anaerobic condition for enhanced biological phosphorus removal. As anoxic condition persist with nitrification occurring during the react period, no phosphorus accumulation occurred by PAOs.

4.6. Discussion

The PSBR was operated with a HRT of 12hr with 11hr of react time, where reactor 1 and 2 were illuminated artificially with a constant light intensity of 35-30 $\mu\text{mol}/\text{m}^2/\text{sec}$. In Phase 2b, after 7hr of react time in Reactor 1, the pH was kept uncontrolled, it was observed that increasing the light intensity to 95-100 $\mu\text{mol}/\text{m}^2/\text{sec}$ led to increase in achieving pH at the end of react period from 8.5 pH to 9pH. Therefore increasing the light intensity was warranted to achieve an increase to pH 9 (removal efficiency: 74.3% \pm 19%) where the removal efficiency was significantly higher than pH8.3 (removal efficiency: 25.6% \pm 7%). The other 12hr where anoxic condition prevailed, the reactors were kept unilluminated and no mixing was done. However, in general the high rate algae ponds (HRAP) where it is been illuminated by sunlight the intensity varies during the day. The experimental study highlighted that high light intensity was required to increase the pH during the latter part of the react cycle when ammonia and carbonate concentrations are low which would enable preferable condition for calcium phosphate precipitation to occur efficiently. Whereas in HRAP, sunlight intensity is higher during the middle course of the light phase. Therefore HRAP due to uncontrolled light intensity condition which may vary during the course of the day and weather condition are not a preferable option to carry out phosphorus removal using algae bacteria consortium. The operational cycle warrants a controlled light intensity using artificial illumination for the phosphorus removal to occur.

The light availability was found to be an important factor in PSBR. Higher concentration led to high light attenuation inside the reactor. Therefore calculating minimum SRT was very important to maintain low reactor concentration and increase the energy efficiency of the system. The minimum SRT calculated was 12days but a SRT of 20days was kept to increase the concentration of nitrifying biomass in the reactor and achieving high ammonia removal rate mostly through nitrification. Since the objective was to study the effect on nitrifying biomass due to pH increase. Therefore, SRT was kept high to allow significant nitrification in the reactor considering the low energy efficiency of the reactor.

For biologically and chemically induced phosphorus precipitation in PSBR to occur at the end of react period with minimum alkalinity and negligible ammonia concentration. A HRT of 12hr is required having react time of 7hr with controlled pH of 7.3, whereas 4hr of uncontrolled pH is kept to increase the pH biologically. The concentration of the influent should also be within a range as shown below:

Ammonia: Upto $50\text{mgNH}_4^+/\text{L/hr}$
Alkalinity: Minimum $1500\text{mg CaCO}_3/\text{L}$ upto $1600\text{ CaCO}_3/\text{L}$

The PSBR with the above condition will require 11hr of react time. When the ammonia concentration is low the react time can be reduced based on the ammonia removal rate calculated during the study period. The PSBR requires high alkalinity in the reactor for the biologically induced precipitation to occur. Since the SRT is high it led to high bicarbonate consumption due to photosynthesis in the reactor by the algae even though the light attenuation was high. Therefore if the biomass in the PSBR had high concentration of nitrifying biomass, minimum SRT can be maintained in the reactor achieving significant ammonium removal. This could led to low algae concentration in reactor hence lower alkalinity in the influent will be required to achieve biologically induced precipitation.

Phosphorus removal through precipitation as struvite (magnesium ammonium phosphate) by dosing magnesium chloride will require ammonium in the mixed liquor at the end of react stage. During the latter part of the reactor when the pH is kept uncontrolled, the alkalinity is low. Therefore the presence of ammonia initiates nitrification process leading to pH decrease as shown in Figure 23 thus hindering the biological increase of pH in the reactor. Thus phosphorus removal by dosing calcium chloride was the preferred option.

In this study chemical phosphorus removal was carried out by dosing Calcium Chloride when suitable condition for phosphorus removal was achieved biologically in PSBR. However, the phosphorus removal can also be carried out by phosphorus accumulating organism (PAOs) in the PSBR. The PAOs require anaerobic and aerobic cycle inside the PSBR which was not observed during the study period. Since aerobic-anoxic cycle prevailed. The anoxic cycle in the PSBR can be converted to anaerobic cycle by dosing sodium acetate to provide enough organic carbon source to denitrify the nitrates in PSBR. This will led to operational complexity and lower efficiency as dosing overestimated sodium acetate will increase COD in PSBR. This will increase the oxygen requirement and also increase the bio mass inside the reactor. Thus reducing the light availability inside the reactor.

CHAPTER

5. Conclusions and Recommendations

5.1. Conclusions

The experiment conducted during the entire study period presented valuable data in removing phosphorus via chemically and biologically induced precipitation of calcium phosphate from synthetic wastewater (Modified BG-11) similar to the effluent of anaerobic digester.

The nitrogen removal was successfully carried out in algae bacteria consortium using red LED light as illuminating source. There was no decrease in nitrification rate observed in the reactor when the pH was increased biologically for phosphorus precipitation to occur as calcium phosphate. Illuminating the photo bioreactor with red led light to oxygenate the reactor using the high 600-700nm spectrum dependency of Chlorophyll-a in an energy efficient manner. An ammonium removal rate of 2.25 to 2.5 mg N-NH₃/L/hr was observed on an average in the both the reactor. There was no negative effect observed in the nitrifying biomass when in the previous cycle the pH was increased to 8.5-9 for the phosphorus precipitation to occur. The pH was increased biologically by switching off pH controller after maintaining a controlled pH for 7hrs in Reactor 1. At the end of react period a pH of 8.5 was achieved, after dosing calcium chloride, phosphorus removal efficiency of 25.64% \pm 7% was observed. The increase in led light intensity from 35-30 μ mol/m²/sec to 95-100 μ mol/m²/sec after 7hr of react time led to biological pH increase of 9. At a pH of 9, the phosphate removal efficiency was 74.31% \pm 19% indicating a significant increase in removal efficiency. However, the removal efficiency should still be increased if the calcium chloride was dosed when pH controller was switched off. This would led to higher contact time of phosphate with calcium hence with the same removal rate, higher calcium phosphate precipitation could occur.

Maintaining a high calcium concentration at the start of reactor meant high calcite formation occurring due to significant alkalinity in the influent, thus less removal efficiency of phosphate as calcium phosphate was observed. The use of LED light as oxygenating source in photo bioreactor make is very suitable for its submerged usage, thus negating the PSBR surface area constraint for light requirement. Also it will consume less electricity as compared to air blowers used in typical SBR processes.

5.2. Recommendations

The objectives of the research study were achieved, however there can be several improvements which can be implemented to effectively remove the nutrients in the PSBR with less control required in the pH and lower operational cost. Some of the recommendations are suggested below:

1. Step feeding the reactor for 6hr in the initial 11hr of react time to control the pH in the nitrification range without the use of acid will be an efficient way of utilizing the bicarbonates in the mixed liquor.
2. The reactor could be illuminated with blue light and red light in 4(red):1(blue) to increase the system efficiency to oxygenate the mixed liquor.
3. Possibilities should also be explored to come up with less energy intensive methods for mixing the PSBR. The solution which can be explored could be the step feed of the reactor from bottom thus agitating the sludge intermittently.
4. The algae used in the PSBR could be inoculated with pure culture of algae with low growth (species such as *Nannochloropsis*) enough to ensure oxygenation of PSBR. This could lead to higher concentration of nitrifying biomass as high SRT could be achieved and lower operation cost arising from less sludge wastage.
5. Machine learning could be implemented in engineered ecosystem such as PSBR to understand and operate the system.

6. REFERENCES

- AITCHISON, P. A., & BUTT, V. S. (1973). The Relation between the Synthesis of Inorganic Polyphosphate and Phosphate Uptake by *Chlorella vulgaris*. *Journal of Experimental Botany*, 24(3), 497–510. <http://doi.org/10.1093/jxb/24.3.497>
- ALFRED C. REDFIELD. (1958). THE BIOLOGICAL CONTROL OF CHEMICAL FACTORS IN THE ENVIRONMENT. *Source: American Scientist*, 46(3), 230–205. Retrieved from <http://www.jstor.org/stable/27827150>
- Amin, S. A., Parker, M. S., & Armbrust, E. V. (2012, September). Interactions between diatoms and bacteria. <http://doi.org/10.1128/MMBR.00007-12>
- Atlas, E., Culberson, C., & Pytkowicz, R. M. (1976). Phosphate association with Na⁺, Ca²⁺ and Mg²⁺ in seawater. *Marine Chemistry*, 4(3), 243–254. [http://doi.org/10.1016/0304-4203\(76\)90011-6](http://doi.org/10.1016/0304-4203(76)90011-6)
- Barat, R., Montoya, T., Seco, A., & Ferrer, J. (2011). Modelling biological and chemically induced precipitation of calcium phosphate in enhanced biological phosphorus removal systems. *Water Research*, 45(12), 3744–3752. <http://doi.org/10.1016/j.watres.2011.04.028>
- Bell, W., & Mitchell, R. (1972). Chemotactic and Growth Responses of Marine Bacteria to Algal Extracellular Products. *Biological Bulletin*, 143(2), 265. <http://doi.org/10.2307/1540052>
- Benemann, J. (2013). Microalgae for Biofuels and Animal Feeds. *Energies*, 6(11), 5869–5886. <http://doi.org/10.3390/en6115869>
- Boelee, N. C., Temmink, H., Janssen, M., Buisman, C. J. N., & Wijffels, R. H. (2011). Nitrogen and phosphorus removal from municipal wastewater effluent using microalgal biofilms. *Water Research*, 45(18), 5925–5933. <http://doi.org/10.1016/j.watres.2011.08.044>
- Brembu, T., Winge, P., Tooming-Klunderud, A., Nederbragt, A. J., Jakobsen, K. S., & Bones, A. M. (2014). The chloroplast genome of the diatom *Seminavis robusta*: New features introduced through multiple mechanisms of horizontal gene transfer. *Marine Genomics*, 16, 17–27. <http://doi.org/10.1016/j.margen.2013.12.002>
- Brown, N., & Shilton, A. (2014). Luxury uptake of phosphorus by microalgae in waste stabilisation ponds: current understanding and future direction. *Reviews in Environmental Science and Bio/Technology*, 13(3), 321–328. <http://doi.org/10.1007/s11157-014-9337-3>
- Bruke, D. A. (n.d.). Removal and Recovery of Phosphate from Liquid Stream.
- Carney, L. T., Reinsch, S. S., Lane, P. D., Solberg, O. D., Jansen, L. S., Williams, K. P., ... Lane, T. W. (2014). Microbiome analysis of a microalgal mass culture growing in municipal wastewater in a prototype OMEGA photobioreactor. *Algal Research*, 4, 52–61. <http://doi.org/10.1016/j.algal.2013.11.006>
- Cembella, A. D., Antia, N. J., & Harrison, P. J. (1982). The Utilization of Inorganic and Organic Phosphorous Compounds as Nutrients by Eukaryotic Microalgae: A Multidisciplinary Perspective: Part I. *CRC Critical Reviews in Microbiology*, 10(4), 317–391. <http://doi.org/10.3109/10408418209113567>
- Cembella, A. D., Antia, N. J., Harrison, P. J., & Rhee, G.-Y. (1984). The Utilization of Inorganic and Organic Phosphorous Compounds as Nutrients by Eukaryotic Microalgae: A Multidisciplinary Perspective: Part 2. *CRC Critical Reviews in Microbiology*, 11(1), 13–81. <http://doi.org/10.3109/10408418409105902>
- Chaiwong, C. (n.d.). *Evaluation of Photobioreactor Coupled in Cess-To-Fit Model for Treating Blackwater*.
- Chave, K. E., & Suess, E. (1970). CALCIUM CARBONATE SATURATION IN SEAWATER: EFFECTS OF DISSOLVED ORGANIC MATTER¹. *Limnology and Oceanography*, 15(4), 633–637. <http://doi.org/10.4319/lo.1970.15.4.0633>
- Claros, J., Jiménez, E., Aguado, D., Ferrer, J., Seco, A., & Serralta, J. (2013). Effect of pH and HNO₂ concentration on the activity of ammonia-oxidizing bacteria in a partial

- nitritation reactor. *Water Science & Technology*, 67(11), 2587. <http://doi.org/10.2166/wst.2013.132>
- Croft, M. T., Lawrence, A. D., Raux-Deery, E., Warren, M. J., & Smith, A. G. (2005). Algae acquire vitamin B12 through a symbiotic relationship with bacteria. *Nature*, 438(7064), 90–3. <http://doi.org/10.1038/nature04056>
- de-Bashan, L. E., Hernandez, J.-P., Morey, T., & Bashan, Y. (2004). Microalgae growth-promoting bacteria as “helpers” for microalgae: a novel approach for removing ammonium and phosphorus from municipal wastewater. *Water Research*, 38(2), 466–474. <http://doi.org/10.1016/j.watres.2003.09.022>
- DeRidder, M., Jong, S. de, Polchar, J., & Lingemann, and S. (2012). Risks and Opportunities in the Global Phosphate Rock Market, 1–101. <http://doi.org/Report No 17/12/12>, ISBN/EAN: 978-94-91040-69-6
- Driver, J., Lijmbach, D., & Steen, I. (1999). Why Recover Phosphorus for Recycling, and How? *Environmental Technology*, 20(7), 651–662. <http://doi.org/10.1080/09593332008616861>
- Eixler, S., Karsten, U., & Selig, U. (2006). Phosphorus storage in *Chlorella vulgaris* (Trebouxiophyceae, Chlorophyta) cells and its dependence on phosphate supply. *Phycologia*, 45(1), 53–60. <http://doi.org/10.2216/04-79.1>
- Escapa, C., Coimbra, R. N., Paniagua, S., García, A. I., & Otero, M. (2015). Nutrients and pharmaceuticals removal from wastewater by culture and harvesting of *Chlorella sorokiniana*. *Bioresource Technology*, 185, 276–284. <http://doi.org/10.1016/j.biortech.2015.03.004>
- Fredy, D. (2013). *Nitrification and denitrification by algal-bacterial biomass in a Sequential Batch Photo-bioreactor: effect of SRT*. UNESCO-IHE, Delft.
- Goecke, F., Labes, A., Wiese, J., & Imhoff, J. (2010). Chemical interactions between marine macroalgae and bacteria. *Marine Ecology Progress Series*, 409, 267–299. <http://doi.org/10.3354/meps08607>
- González, C., Marciniak, J., Villaverde, S., García-Encina, P. A., & Muñoz, R. (2008). Microalgae-based processes for the biodegradation of pretreated piggery wastewaters. *Applied Microbiology and Biotechnology*, 80(5), 891–898. <http://doi.org/10.1007/s00253-008-1571-6>
- Gonzalez, L. E., & Bashan, Y. (2000). Increased Growth of the Microalga *Chlorella vulgaris* when Coimmobilized and Cocultured in Alginate Beads with the Plant-Growth-Promoting Bacterium *Azospirillum brasilense*. *Applied and Environmental Microbiology*, 66(4), 1527–1531. <http://doi.org/10.1128/AEM.66.4.1527-1531.2000>
- Grases, F., & March, J. G. (1990). Determination of phosphate based on inhibition of crystal growth of calcite. *Analytica Chimica Acta*, 229, 249–254. [http://doi.org/10.1016/S0003-2670\(00\)85135-1](http://doi.org/10.1016/S0003-2670(00)85135-1)
- Green, F. B., Bernstone, L. S., Lundquist, T. J., & Oswald, W. J. (1996). Advanced integrated wastewater pond systems for nitrogen removal. *Water Science and Technology*, 33(7).
- Haandel, A. van, & Lubbe, J. van der. (2007). *Handbook biological waste water treatment : design and optimisation of activated sludge systems*. Quist.
- Hartley, A. M., House, W. A., Callow, M. E., & Leadbeater, B. S. C. (1997). Coprecipitation of phosphate with calcite in the presence of photosynthesizing green algae. *Water Research*, 31(9), 2261–2268. [http://doi.org/10.1016/S0043-1354\(97\)00103-6](http://doi.org/10.1016/S0043-1354(97)00103-6)
- Henze, M., Ekama, M. B. (2008). *Biological Wastewater Treatment*.
- Jiménez, E., Giménez, J. B., Ruano, M. V., Ferrer, J., & Serralta, J. (2011). Effect of pH and nitrite concentration on nitrite oxidation rate. *Bioresource Technology*, 102(19), 8741–8747. <http://doi.org/10.1016/j.biortech.2011.07.092>
- John F. Ferguson, D. J. and J. E. (1973). Calcium phosphate precipitation at slightly alkaline pH values. *Journal (Water Pollution Control Federation)*, Vol. 45(No. 4), 620–631.
- Joko, I. (1985). Phosphorus Removal from Wastewater by the Crystallization Method. *Water*

- Science and Technology*, 17(2–3), 121–132.
- Karya, N. G. A. I., Van Der Steen, N. P., & Lens, P. N. L. (2013). Photo-oxygenation to support nitrification in an algal–bacterial consortium treating artificial wastewater. *Bioresource Technology*, 134, 244–250. <http://doi.org/10.1016/j.biortech.2013.02.005>
- Kebede-Westhead, E., Pizarro, C., & Mulbry, W. W. (2006). Treatment of swine manure effluent using freshwater algae: Production, nutrient recovery, and elemental composition of algal biomass at four effluent loading rates. *Journal of Applied Phycology*, 18(1), 41–46. <http://doi.org/10.1007/s10811-005-9012-8>
- Koutsoukos, P., Amjad, Z., Tomson, M. B., & Nancollas, G. H. (1979). Crystallization of Calcium Phosphates. A Constant Composition Study. *Journal of the American Chemical Society*, 1553–1557. <http://doi.org/10.1021/ja00525a015>
- Krohn-Molt, I., Wemheuer, B., Alawi, M., Poehlein, A., Gullert, S., Schmeisser, C., ... Streit, W. R. (2013). Metagenome Survey of a Multispecies and Alga-Associated Biofilm Revealed Key Elements of Bacterial-Algal Interactions in Photobioreactors. *Applied and Environmental Microbiology*, 79(20), 6196–6206. <http://doi.org/10.1128/AEM.01641-13>
- Li, C., Ju, L.-K., Telling, R. C., Nigam, P. S., Mussnug, J. H., Posten, C., ... Hankamer, B. (2014). Conversion of wastewater organics into biodiesel feedstock through the predator-prey interactions between phagotrophic microalgae and bacteria. *RSC Adv.*, 4(83), 44026–44029. <http://doi.org/10.1039/C4RA06374K>
- Lin, Y.-P., & Singer, P. C. (2005). Inhibition of calcite crystal growth by polyphosphates. *Water Research*, 39(19), 4835–4843. <http://doi.org/10.1016/j.watres.2005.10.003>
- Mara, D. (2003). *Domestic Wastewater Treatment in Developing Countries*.
- Martín, H. G., Ivanova, N., Kunin, V., Warnecke, F., Barry, K. W., McHardy, A. C., ... Hugenholtz, P. (2006). Metagenomic analysis of two enhanced biological phosphorus removal (EBPR) sludge communities. *Nature Biotechnology*, 24(10), 1263–1269. <http://doi.org/10.1038/nbt1247>
- Miyachi, S., Kanai, R., Mihara, S., Miyachi, S., & Aoki, S. (1964). Metabolic roles of inorganic polyphosphates in chlorella cells. *Biochimica et Biophysica Acta (BBA) - General Subjects*, 93(3), 625–634. [http://doi.org/10.1016/0304-4165\(64\)90345-9](http://doi.org/10.1016/0304-4165(64)90345-9)
- MIYACHI, S., & MIYACHI, S. (1961). MODES OF FORMATION OF PHOSPHATE COMPOUNDS AND THEIR TURNOVER IN CHLORELLA CELLS DURING THE PROCESS OF LIFE CYCLE AS STUDIED BY THE TECHNIQUE OF SYNCHRONOUS CULTURE. *Plant and Cell Physiology*, 2(4), 415–424.
- Muñoz, R., & Guieysse, B. (2006). Algal–bacterial processes for the treatment of hazardous contaminants: A review. *Water Research*, 40(15), 2799–2815. <http://doi.org/10.1016/j.watres.2006.06.011>
- Olguín, E. J. (2012). Dual purpose microalgae–bacteria-based systems that treat wastewater and produce biodiesel and chemical products within a Biorefinery. *Biotechnology Advances*, 30(5), 1031–1046. <http://doi.org/10.1016/j.biotechadv.2012.05.001>
- Park, J., Seo, J., & Kwon, E. E. (2012). Microalgae Production Using Wastewater: Effect of Light-Emitting Diode Wavelength on Microalgal Growth. *Environmental Engineering Science*, 29(11), 995–1001. <http://doi.org/10.1089/ees.2012.0082>
- Posadas, E., Bochon, S., Coca, M., García-González, M. C., García-Encina, P. A., & Muñoz, R. (2014). Microalgae-based agro-industrial wastewater treatment: a preliminary screening of biodegradability. *Journal of Applied Phycology*, 26(6), 2335–2345. <http://doi.org/10.1007/s10811-014-0263-0>
- Powell, N., Shilton, A., Chisti, Y., & Pratt, S. (2009). Towards a luxury uptake process via microalgae – Defining the polyphosphate dynamics. *Water Research*, 43(17), 4207–4213. <http://doi.org/10.1016/j.watres.2009.06.011>
- Powell, N., Shilton, A. N., Pratt, S., & Chisti, Y. (2006). Luxury uptake of phosphorus by microalgae in waste stabilisation ponds. *3rd Young Researchers Conference (YRC06)*.
- Powell, N., Shilton, A., Pratt, S., & Chisti, Y. (2011). Luxury uptake of phosphorus by

- microalgae in full-scale waste stabilisation ponds. *Water Science & Technology*, 63(4), 704. <http://doi.org/10.2166/wst.2011.116>
- Rasala, B. A., & Mayfield, S. P. (2015). Photosynthetic biomanufacturing in green algae; production of recombinant proteins for industrial, nutritional, and medical uses. *Photosynthesis Research*, 123(3), 227–239. <http://doi.org/10.1007/s11120-014-9994-7>
- Rawat, I., Ranjith Kumar, R., Mutanda, T., & Bux, F. (2013). Biodiesel from microalgae: A critical evaluation from laboratory to large scale production. *Applied Energy*, 103, 444–467. <http://doi.org/10.1016/j.apenergy.2012.10.004>
- Reddy, M. M. (1977). Crystallization of calcium carbonate in the presence of trace concentrations of phosphorus-containing anions. *Journal of Crystal Growth*, 41(2), 287–295. [http://doi.org/10.1016/0022-0248\(77\)90057-4](http://doi.org/10.1016/0022-0248(77)90057-4)
- Solovchenko, A., Verschoor, A. M., Jablonowski, N. D., & Nedbal, L. (2016). Phosphorus from wastewater to crops: An alternative path involving microalgae. *Biotechnology Advances*. <http://doi.org/10.1016/j.biotechadv.2016.01.002>
- Song, Y., Hahn, H. H., & Hoffmann, E. (2002). Effects of solution conditions on the precipitation of phosphate for recovery: A thermodynamic evaluation. *Chemosphere*, 48(10), 1029–1034. [http://doi.org/10.1016/S0045-6535\(02\)00183-2](http://doi.org/10.1016/S0045-6535(02)00183-2)
- Song, Y., Hahn, H. H., & Hoffmann, E. (2002). The effect of carbonate on the precipitation of calcium phosphate. *Environmental Technology*, 23(2), 207–215. <http://doi.org/10.1080/09593332508618427>
- Spanjers, H., Vanrolleghem, P., Olsson, G., & Dold, P. (1996). Respirometry in control of the activated sludge process. *Water Science and Technology*, 34(3–4), 117–126.
- Stumm, W., & Morgan, J. J. (1996). *Aquatic chemistry: chemical equilibria and rates in natural waters*. Wiley.
- United Nations Environment Programme. (2011). *UNEP 2011 Year Book*. Retrieved from http://hqweb.unep.org/yearbook/2011/pdfs/UNEP_YEARBOOK_Fullreport.pdf
- van der Weijden, R. D., van der Heijden, A. E., Witkamp, G. J., & van Rosmalen, G. M. (1997). The influence of total calcium and total carbonate on the growth rate of calcite. *Journal of Crystal Growth*, 171(1), 190–196. [http://doi.org/10.1016/S0022-0248\(96\)00487-3](http://doi.org/10.1016/S0022-0248(96)00487-3)
- Wang, M., Yang, H., Ergas, S. J., & Van Der Steen, P. (2015). A novel shortcut nitrogen removal process using an algal-bacterial consortium in a photo-sequencing batch reactor (PSBR). *Water Research*, 87, 38–48. <http://doi.org/10.1016/j.watres.2015.09.016>
- Wilfert, P., Kumar, P. S., Korving, L., Witkamp, G.-J., & van Loosdrecht, M. C. M. (2015). The Relevance of Phosphorus and Iron Chemistry to the Recovery of Phosphorus from Wastewater: A Review. *Environmental Science & Technology*, 49(16), 9400–14. <http://doi.org/10.1021/acs.est.5b00150>
- Willén, E. (1987). Phytoplankton and reversed Eutrophication in Lake Mälaren, Central Sweden, 1965–1983. *British Phycological Journal*, 22(2), 193–208. <http://doi.org/10.1080/00071618700650241>
- Wu, Y.-H., Hu, H.-Y., Yu, Y., Zhang, T.-Y., Zhu, S.-F., Zhuang, L.-L., ... Lu, Y. (2014). Microalgal species for sustainable biomass/lipid production using wastewater as resource: A review. *Renewable and Sustainable Energy Reviews*, 33, 675–688. <http://doi.org/10.1016/j.rser.2014.02.026>

7. APPENDIX 1

Alkalinity consumption in Phase 1 of Reactor 1 and 2

ID	Time	Vol of 0.1 HCL, V_x	Measured Alkalinity, Alk_{meas}	Alkalinity Consumed, $(V_x \cdot C_{ab}) \cdot 50$	Actual Alkalinity of the Sample, Alk_{act} (mg $CaCO_3/L$)	Alkalinity Consumed	Alkalinity Consumed per Hour
R1-B1-0	0	0	480	0	480		
R1-B1-3	3	8	270	40	310	170	56.67
R1-B1-6	6	4	65	20	85	225	75.00
R2-B1-0	0	0	515	0	515		
R2-B1-3	3	10	315	50	365	150	50.00
R2-B1-6	6	5	135	25	160	205	68.33
R1-B2-0	0	0	535	0	535		
R1-B2-2	2	20	250	100	350	185	92.50
R1-B2-4	4	15	110	75	185	165	82.50
R1-B2-6	6	10	50	50	100	85	42.50
R2-B2-0	0	0	405	0	405		
R2-B2-2	2	5	210	25	235	170	85.00
R2-B2-4	4	5	130	25	155	80	40.00
R2-B2-6	6	3	80	15	95	60	30.00
R1-B3-0	0	0	880	0	880		
R1-B3-2	2	60	280	300	580	300	150.00
R1-B3-4	4	30	260	150	410	170	85.00
R1-B3-6	6	20	130	100	230	180	90.00
R2-B3-0	0	0	830	0	830		
R2-B3-2	2	30	440	150	590	240	120.00
R2-B3-4	4	20	160	100	260	330	165.00
R2-B3-6	6	10	80	50	130	130	65.00

Alkalinity consumption in Phase 2a of Reactor 1 and 2

ID	Time	Vol of 0.1 HCL, V_x	Measured Alkalinity, Alk_{meas}	Alkalinity Consumed, $(V_x \cdot C_{ab}) \cdot 50$	Actual Alkalinity of the Sample, Alk_{act} (mg $CaCO_3/L$)	Alkalinity Consumed	Alkalinity Consumed per Hour
R1-C1-0	0	0	420	0	420		
R1-C1-2	2	10	110	50	160	260	130.00
R1-C1-4	4	5	50	25	75	85	42.50
R2-C1-0	0	0	380	0	380		
R2-C1-2	2	15	150	75	225	155	77.50
R2-C1-4	4	5	70	25	95	130	65.00
R1-C2-0	0	0	570	0	570		
R1-C2-2	2	10	240	50	290	280	140.00
R1-C2-4	4	5	100	25	125	165	82.50
R1-C2-6	6	3	50	15	65	60	30.00
R2-C2-0	0	0	610	0	610		
R2-C2-2	2	25	240	125	365	245	122.50
R2-C2-4	4	20	100	100	200	165	82.50
R2-C2-6	6	10	70	50	120	80	40.00
R1-C3-0	0	0	460	0	460		
R1-C3-2	2	5	280	25	305	155	77.50
R1-C3-4	4	5	200	25	225	80	40.00
R1-C3-6	6	3	70	15	85	140	70.00
R2-C3-0	0	0	470	0	470		
R2-C3-2	2	10	370	50	420	50	25.00
R2-C3-4	4	5	170	25	195	225	112.50
R2-C3-6	6	3	120	15	135	60	30.00

Alkalinity consumption in Phase 2b of Reactor 1 and 2

ID	Time	Vol of 0.1 HCL, V_x	Total Alkalinity, alk_x	Alkalinity Consumed, $V_x \cdot C_{ab}$	Actual Alkalinity of the Sample, V_e .C _a (mg CaCO ₃ /L)	Alkalinity Consumed	Alkalinity Consumed per Hour
R2-D1-0	0	0	920	0	920		
R2-D1-1	1	20	740	100	840	80	80
R2-D1-2	2	15	650	75	725	115	115
R2-D1-4	4	11	550	55	605	120	60
R2-D1-6	6	10	370	50	420	185	92
R2-D2-0	0	0	920	0	920		
R2-D2-1	1	14	740	70	810	110	110
R2-D2-2	2	15	650	75	725	85	85
R2-D2-4	4	7	550	35	585	140	70
R2-D2-6	6	9	370	45	415	170	85
R2-D3-0	0	0	920	0	920		
R2-D3-1	1	19	750	95	845	75	75
R2-D3-2	2	15	680	75	755	90	90
R2-D3-4	4	10	360	50	410	345	173
R2-D3-6	6	7	290	35	325	85	42
R2-D5-0	0	0	820	0	820		
R2-D5-1	1	16	730	80	810	10	10
R2-D5-2	2	16	580	80	660	150	150
R2-D5-4	4	10	390	50	440	220	110
R2-D5-6	6	12	300	60	360	80	40
R2-D6-0	0	0	890	0	890		
R2-D6-1	1	20	780	100	880	10	10
R2-D6-2	2	14	550	70	620	260	260
R2-D6-4	4	11	410	55	465	155	77
R2-D6-6	6	6	350	30	380	85	43